

Supporting information for

Effective targeting on proton transfer at ground and excited states of *ortho*-(2'-imidazolyl)naphthol constitutional isomers

Preparation of <i>ortho</i> -hydroxynaphthoate esters.....	3
Preparation of <i>ortho</i> -hydroxy(4,5-dihydro-1 <i>H</i> -imidazol-2-yl)naphthalenes.....	3
Preparation of <i>ortho</i> -(1 <i>H</i> -imidazol-2-yl)naphthols.....	4
Fig. S1. ¹ H NMR spectrum for 2-hydroxy-1-naphthoate esters (2a)	6
Fig. S2. ¹ H NMR spectrum for 1-hydroxy-2-naphthoate esters (2b)	7
Fig. S3. ¹ H NMR spectrum for 3-hydroxy-2-naphthoate esters (2c)	8
Fig. S4. NMR spectra for 1-(4,5-dihydro-1 <i>H</i> -imidazol-2-yl)naphthalen-2-ol (3a).....	9
Fig. S5. NMR spectra for 2-(4,5-dihydro-1 <i>H</i> -imidazol-2-yl)naphthalen-1-ol (3b)	10
Fig. S6. NMR spectra for 3-(4,5-dihydro-1 <i>H</i> -imidazol-2-yl)naphthalen-2-ol (3c).....	11
Fig. S7. NMR spectra for 1-(1 <i>H</i> -imidazol-2-yl)naphthalen-2-ol (1NI2OH).....	12
Fig. S8. NMR spectra for 2-(1 <i>H</i> -imidazol-2-yl)naphthalen-1-ol (2NI1OH).....	13
Fig. S9. NMR spectra for 3-(1 <i>H</i> -imidazol-2-yl)naphthalen-2-ol (3NI2OH).....	14
Fig. S10. Spectrophotometric, analytical and statistical data for the pH-titration of 1-(1 <i>H</i> -imidazol-2-yl)naphthalen-2-ol (1NI2OH).	15
Fig. S11. Spectrofluorimetric, analytical and statistical data for the pH-titration of 1-(1 <i>H</i> -imidazol-2-yl)naphthalen-2-ol (1NI2OH).	16
Fig. S12. Spectrophotometric, analytical and statistical data for the pH-titration of 2-(1 <i>H</i> -imidazol-2-yl)naphthalen-1-ol (2NI1OH)	17
Fig. S13. Spectrofluorimetric, analytical and statistical data for the pH-titration of 2-(1 <i>H</i> -imidazol-2-yl)naphthalen-1-ol (2NI1OH)	18
Fig. S14. Spectrophotometric, analytical and statistical data for the pH-titration of 3-(1 <i>H</i> -imidazol-2-yl)naphthalen-2-ol (3NI2OH)	19
Fig. S15. Spectrofluorimetric, analytical and statistical data for the pH-titration of 3-(1 <i>H</i> -imidazol-2-yl)naphthalen-2-ol (3NI2OH)	20
Fig. S16. Determination of the quantum yield (Φ) for 1-(1 <i>H</i> -imidazol-2-yl)naphthalen-2-ol (1NI2OH).	21
Fig. S17. Determination of the quantum yield (Φ) for 2-(1 <i>H</i> -imidazol-2-yl)naphthalen-1-ol (2NI1OH).	22
Fig. S18. Determination of the quantum yield (Φ) for 3-(1 <i>H</i> -imidazol-2-yl)naphthalen-2-ol (3NI2OH)	23
Fig. S19. Absorption and emission spectra for 1-(1 <i>H</i> -imidazol-2-yl)naphthalen-2-ol (1Ni2OH), 2-(1 <i>H</i> -imidazol-2-yl)naphthalen-1-ol (2Ni1OH) and 3-(1 <i>H</i> -imidazol-2-yl)naphthalen-2-ol (3Ni2OH) in different solvents at 25 °C.....	24
Fig. S20. Selected structures along the Potential Energy Surface in the ground state for the rotation around the interannular bond between the naphthol and the imidazole ring of 1NI2OH, 2NI1OH, and 3NI2OH.....	25
Fig. S21. HOMO and LUMO orbital diagrams for optimized structures of 1NI2OH, 2NI1OH, and 3NI2OH in Fig. 4	26

Table S1. Cartesian coordinates for the S_0 - N_{syn} and S_0 -PT forms of 1NI2OH shown in Fig. 4.. 27

Table S2. Cartesian coordinates for the S_1 - N_{syn} and S_1 -PT forms of 1NI2OH shown in Fig. 4.. 28

Table S3. Cartesian coordinates for the S_0 - N_{syn} and S_0 -PT forms of 2NI1OH shown in Fig. 4.. 29

Table S4. Cartesian coordinates for the S_1 - N_{syn} and S_1 -PT forms of 2NI1OH shown in Fig. 4.. 30

Table S5. Cartesian coordinates for the S_0 - N_{syn} and S_0 -PT forms of 3NI2OH shown in Fig. 4.. 31

Table S6. Cartesian coordinates for the S_1 - N_{syn} and S_1 -PT forms of 3NI2OH shown in Fig. 4.. 32

Preparation of *ortho*-hydroxynaphthoate esters (2**, Figures S1-S3).** The procedure was accordingly to a previous report.¹ A mixture of *ortho*-hydroxy-naphthoic acid (15.9 mmol, 1 eq.), KHCO₃ (19.1 mmol, 1.2 eq.) and alkyl iodide (47.7 mmol, 3 eq.) in commercial DMF (24 mL) was heated under magnetic stir at 40 °C for 3 h. The resulting mixture was poured into water (200 mL) and extracted with EtOAc (3x30mL). The organic layer was washed with NaHCO₃ 5% (3x15mL) and water (1x25mL), and dried with anhydrous Na₂SO₄. The ethyl acetate was removed under reduced pressure to give the ester **2**. Yield was usually higher than 85%.

Methyl 2-hydroxy-1-naphthoate (2aMe): orange solid; ¹H NMR (200 MHz, CDCl₃) δ (ppm) 4.06 (3H, s), 7.14 (1H, d, *J* = 9.0 Hz), 7.34 (1H, t, *J* = 7.3 Hz), 7.53 (1H, t, *J* = 7.3 Hz), 7.71 (1H, d, *J* = 7.9 Hz), 7.84 (1H, d, *J* = 9.0 Hz), 8.70 (1H, d, *J* = 8.7 Hz), 12.27 (1H, s).

Ethyl 2-hydroxy-1-naphthoate (2aEt): orange solid; ¹H NMR (200 MHz, CDCl₃) δ (ppm) 1.56 (3H, t, *J* = 7.1 Hz), 4.60 (2H, q, *J* = 7.1 Hz), 7.18 (1H, d, *J* = 9.0 Hz), 7.38 (1H, t, *J* = 7.5 Hz), 7.57 (1H, t, *J* = 7.5 Hz), 7.76 (1H, d, *J* = 8.0 Hz), 7.90 (1H, d, *J* = 8.9 Hz), 8.81 (1H, d, *J* = 8.7 Hz), 12.38 (1H, s).

Methyl 1-hydroxy-2-naphthoate (2bMe): brown solid; ¹H NMR (200 MHz, CDCl₃) δ (ppm) 3.98 (3H, s), 7.26 (1H, d, *J* = 8.6 Hz), 7.46-7.63 (2H, m), 7.75 (2H, d, *J* = 7.7 Hz), 8.40 (1H, br d, *J* = 7.9 Hz), 11.98 (1H, s).

Ethyl 1-hydroxy-2-naphthoate (2bEt): brown solid; ¹H NMR (200 MHz, CDCl₃) δ (ppm) 1.45 (3H, t, *J* = 7.1 Hz), 4.46 (2H, q, *J* = 7.1 Hz), 7.28 (1H, d, *J* = 8.7 Hz), 7.47-7.63 (2H, m), 7.76 (1H, br d, *J* = 7.4 Hz), 7.78 (1H, d, *J* = 8.7 Hz), 8.41 (1H, br d, *J* = 8.0 Hz), 12.08 (1H, s).

Methyl 3-hydroxy-2-naphthoate (2cMe): pale brown solid; ¹H NMR (200 MHz, CDCl₃) δ ppm 4.00 (3H, s), 7.26-7.34 (2H, m), 7.48 (1H, t, *J* = 7.5 Hz), 7.66 (1H, d, *J* = 8.3 Hz), 7.78 (1H, d, *J* = 8.2 Hz), 8.46 (1H, s), 10.42 (1H, s).

Ethyl 3-hydroxy-2-naphthoate (2cEt): pale brown solid; ¹H NMR (200 MHz, CDCl₃) δ ppm 1.50 (3H, t, *J* = 7.1 Hz), 4.50 (2H, q, *J* = 7.1 Hz), 7.29-7.37 (2H, m), 7.51 (1H, t, *J* = 7.0 Hz), 7.70 (1H, d, *J* = 8.3 Hz), 7.82 (1H, d, *J* = 8.3 Hz), 8.50 (1H, s), 10.55 (1H, s).

Preparation of *ortho*-hydroxy(4,5-dihydro-1*H*-imidazol-2-yl)naphthalenes (3**, Figures S4-S6):** The ester **2** (10.2 mmol, 1 eq.) was mixed with distilled ethylenediamine (66.8 mmol, 6 eq.) and refluxed for 6 h. Then, methanol (15 mL) was added to the reaction mixture, and transferred to a fridge for 12 h. A solid was filtered off, washed with cold methanol, and recrystallized in hot

methanol to give about 70% of compound **3**. No attempt was made to isolate the intermediate amide, which seemed to be unstable under this reaction conditions.

1-(4,5-dihydro-1H-imidazol-2-yl)naphthalen-2-ol (3a): yellow crystals, mp 208-210 °C; ¹H NMR (200 MHz, (CD₃)₂SO) δ (ppm) 2.78 (2H, t, *J* = 6.1 Hz), 3.38 (2H, t, *J* = 6.1 Hz), 7.08 (1H, d, *J* = 8.9 Hz), 7.18 (1H, t, *J* = 7.0 Hz), 7.36 (1H, t, *J* = 7.1 Hz), 7.69 (1H, d, *J* = 8.9 Hz), 7.71 (1H, d, *J* = 7.7 Hz), 8.00 (1H, d, *J* = 8.4 Hz), 9.1 (br s); ¹³C NMR and DEPT-135 (50 MHz, (CD₃)₂SO) δ (ppm) 41.2 (CH₂), 41.5 (CH₂), 116.6 (C), 120.9 (CH), 122.1 (CH), 124.2 (CH), 126.7 (CH), 127.0 (C), 128.1 (CH), 130.5 (CH), 132.8 (C), 156.6 (C), 168.7 (C).

2-(4,5-dihydro-1H-imidazol-2-yl)naphthalen-1-ol (3b): yellow crystals, sublimation > 248 °C; ¹H NMR (200 MHz, (CD₃)₂SO) δ (ppm) 3.78 (4H, s), 6.55 (1H, d, *J* = 8.9 Hz), 7.26 (1H, t, *J* = 6.9 Hz), 7.34 (1H, d, *J* = 8.9 Hz), 7.42 (1H, t, *J* = 7.0 Hz), 7.53 (1H, d, *J* = 7.7 Hz), 8.27 (1H, d, *J* = 7.9 Hz), 10.2 (br s); ¹³C NMR and DEPT-135 (50 MHz, (CD₃)₂SO) δ (ppm) 45.0 (CH₂), 110.7 (CH), 125.2 (CH), 126.8 (CH), 127.0 (CH), 128.5 (CH), 130.3 (CH), 133.0 (C), 139.2 (C), 167.3 (C), 175.5 (C).

3-(4,5-dihydro-1H-imidazol-2-yl)naphthalen-2-ol (3c): yellow crystals, mp 205-207 °C; ¹H NMR (200 MHz, (CD₃)₂SO) δ ppm 3.74 (4H, s), 7.23 (1H, s), 7.30 (1H, t, *J* = 7.1 Hz), 7.46 (1H, t, *J* = 7.0 Hz), 7.71 (1H, d, *J* = 8.3 Hz), 7.78 (1H, d, *J* = 8.1 Hz), 8.27 (1H, s), 11.1 (br s); ¹³C NMR and DEPT-135 (50 MHz, (CD₃)₂SO) δ (ppm) 48.4 (CH₂), 110.5 (CH), 114.7 (C), 123.5 (CH), 126.2 (CH), 126.5 (C), 128.1 (CH), 128.5 (CH), 128.7 (CH), 136.0 (C), 157.0 (C), 166.2 (C).

Preparation of *ortho*-(1H-imidazol-2-yl)naphthols (4, Figures S7-S9): The imidazoline **3** (10.4 mmol) was dissolved in diphenyl ether (18.4 mL) under heat. Then, Pd/C 10% (184 mg) was added and the reaction mixture was refluxed for 6 h. The Pd/C was filtered off under reduce pressure while the solution was still hot. To the reaction mixture was added silica gel and washed with petroleum ether (30-60 °C) until complete removal of the diphenyl ether. Silica gel with the adsorbed impure material was poured onto a silica gel column. Chromatography was started in pure chloroform, and a linear gradient until 25% of acetone gave fractions of the pure compound **4**. Yield was about 45 %.

1-(1H-imidazol-2-yl)naphthalen-2-ol (1NI2OH): pale brown crystals, mp 154-156 °C; ¹H NMR (200 MHz, (CD₃)₂CO) δ (ppm) 7.25 (1H, d, *J* = 9.0 Hz), 7.32-7.40 (2H, m), 7.54 (1H, ddd, *J* = 1.4, 7.0 and 8.4 Hz), 7.84 (1H, d, *J* = 9.0 Hz), 7.87 (1H, br d, *J* = 7.6 Hz), 8.35 (1H, br d, *J* =

8.6 Hz); ^{13}C NMR (50 MHz, $(\text{CD}_3)_2\text{CO}$) δ (ppm) 106.4, 119.0, 121.5, 122.9, 123.0, 127.4, 128.4, 128.8, 130.5, 130.7, 144.9, 156.2.

2-(1H-imidazol-2-yl)naphthalen-1-ol (2NI1OH): cyan solid, mp 208-214 °C; ^1H NMR (200 MHz, $(\text{CD}_3)_2\text{CO}$) δ (ppm) 7.27 (2H, s), 7.42 (1H, d, $J = 8.6$ Hz), 7.49-7.56 (2H, m), 7.80-7.85 (1H, m), 7.90 (1H, d, $J = 8.6$ Hz), 8.36-8.41 (1H, m); ^{13}C NMR (50 MHz, $(\text{CD}_3)_2\text{CO}$) δ (ppm) 106.3, 118.3, 121.1, 121.3, 122.7, 125.2, 125.4, 126.9, 127.4, 134.4, 147.1, 153.7.

3-(1H-imidazol-2-yl)naphthalen-2-ol (3NI2OH): pale brown solid, mp 151-153 °C; ^1H NMR (200 MHz, $(\text{CD}_3)_2\text{CO}$), δ ppm 7.22-7.46 (5H, m), 7.75 (2H, t, $J = 8.2$ Hz), 8.38 (1H, s), 12.3 (1H, br s), 12.9 (1H, br s); ^{13}C NMR (50 MHz, $(\text{CD}_3)_2\text{CO}$) δ (ppm) 110.6, 115.8, 123.2, 123.6, 125.9, 127.4, 127.7, 134.9, 146.1, 154.7.

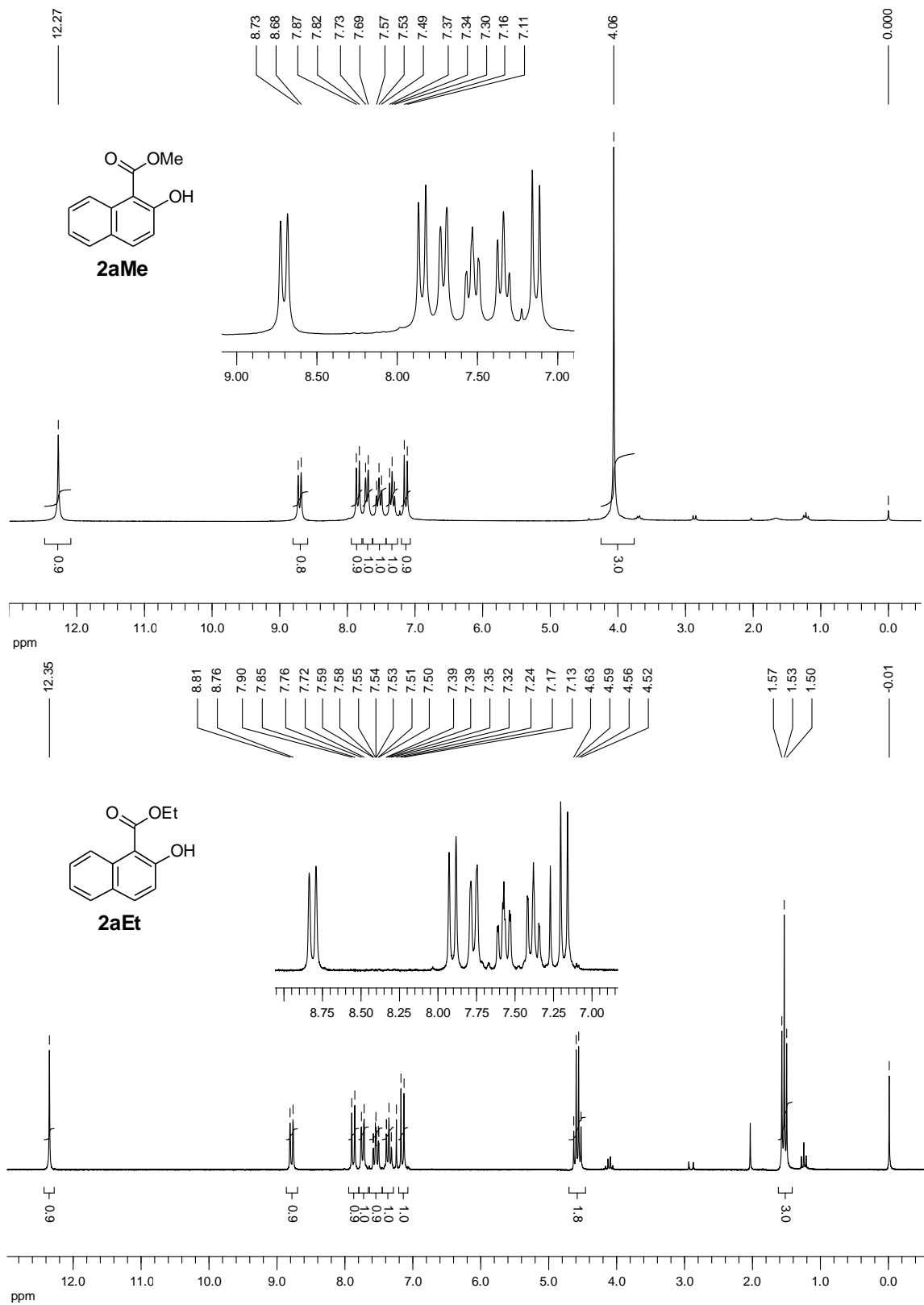


Fig. S1. ^1H NMR spectrum for 2-hydroxy-1-naphthoate esters (**2a**) in CDCl_3 at 200 MHz.

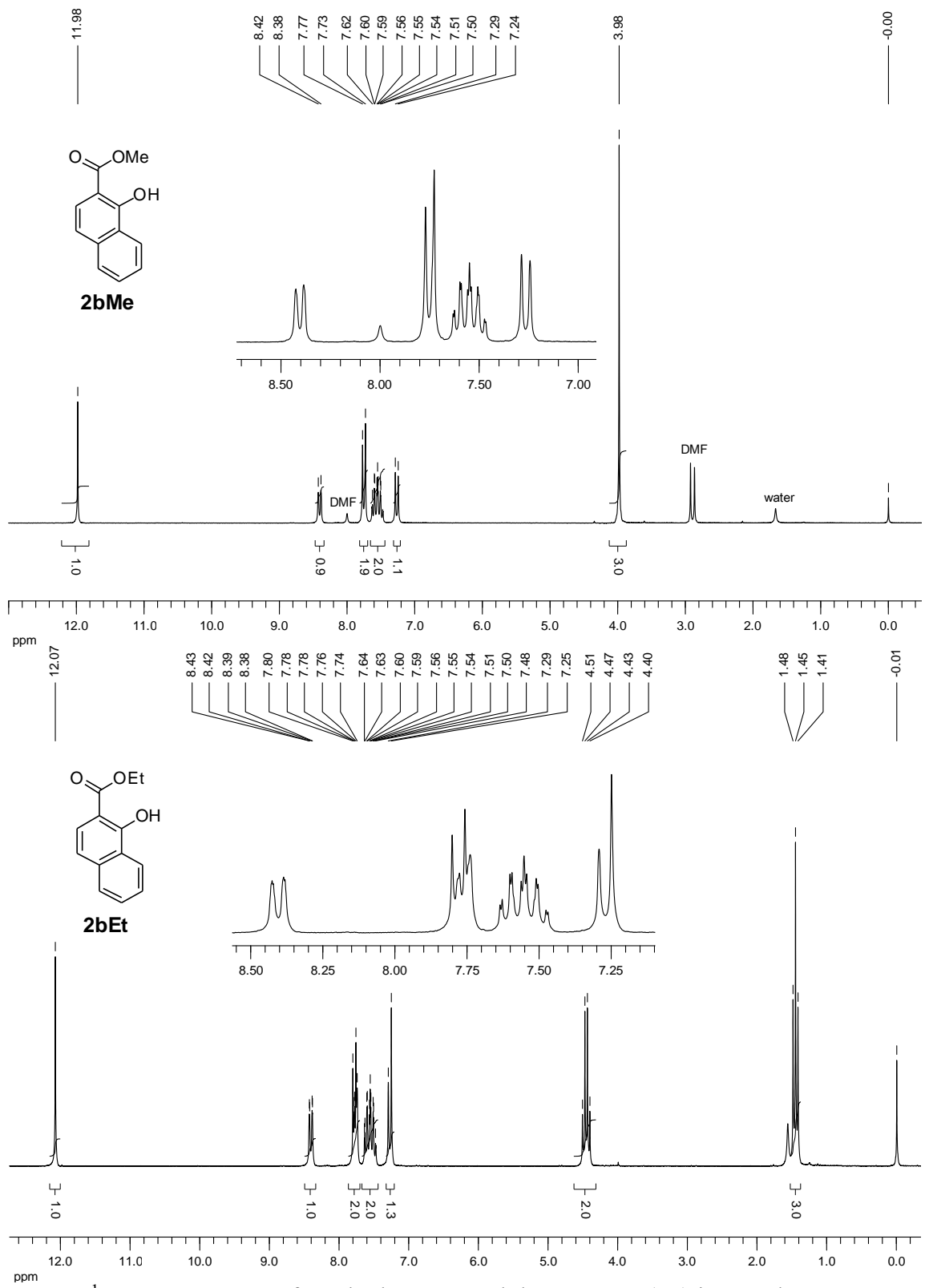


Fig. S2. ^1H NMR spectrum for 1-hydroxy-2-naphthoate esters (**2b**) in CDCl_3 at 200 MHz.

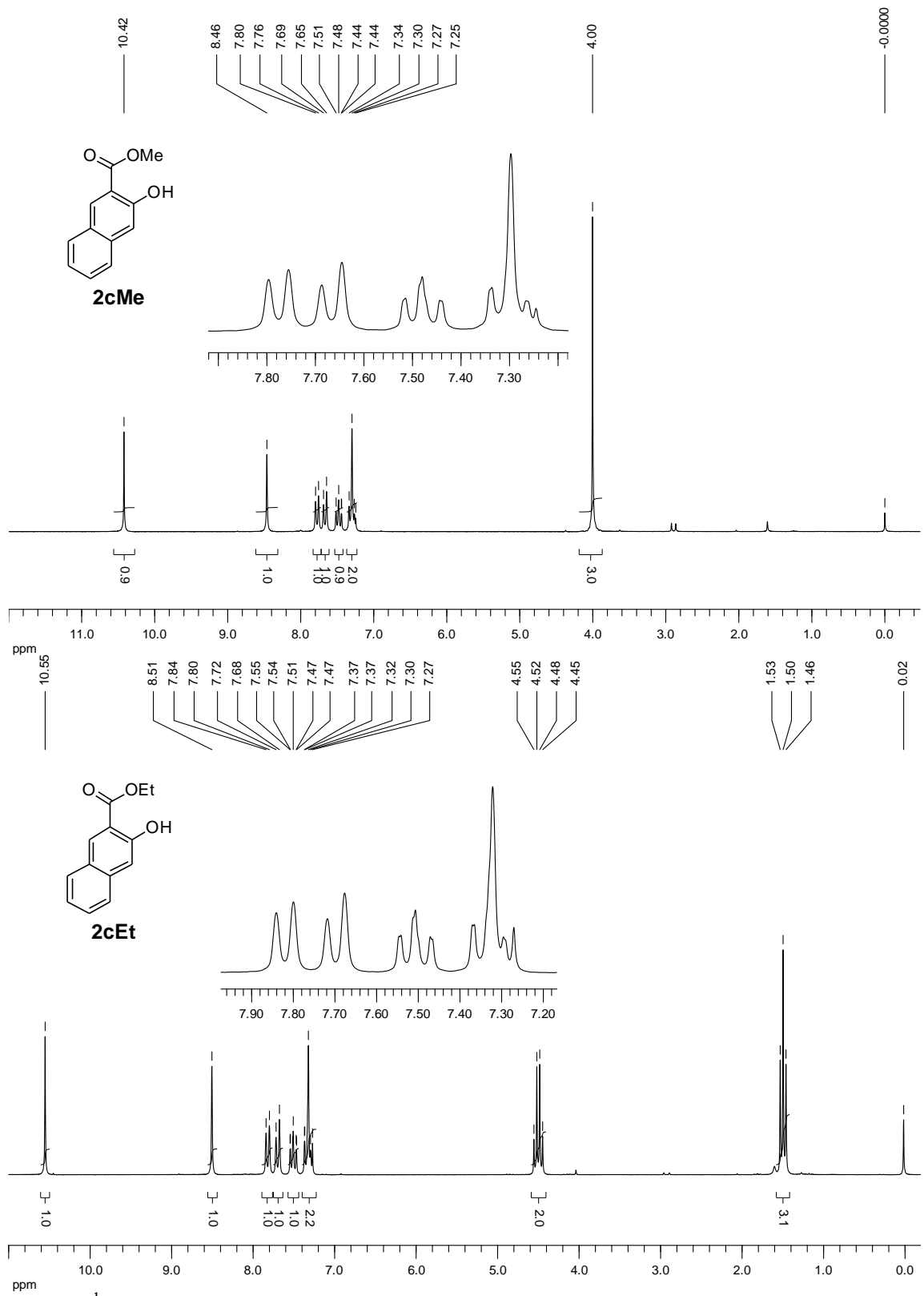


Fig. S3. ^1H NMR spectrum for 3-hydroxy-2-naphthoate esters (**2c**) in CDCl_3 at 200 MHz.

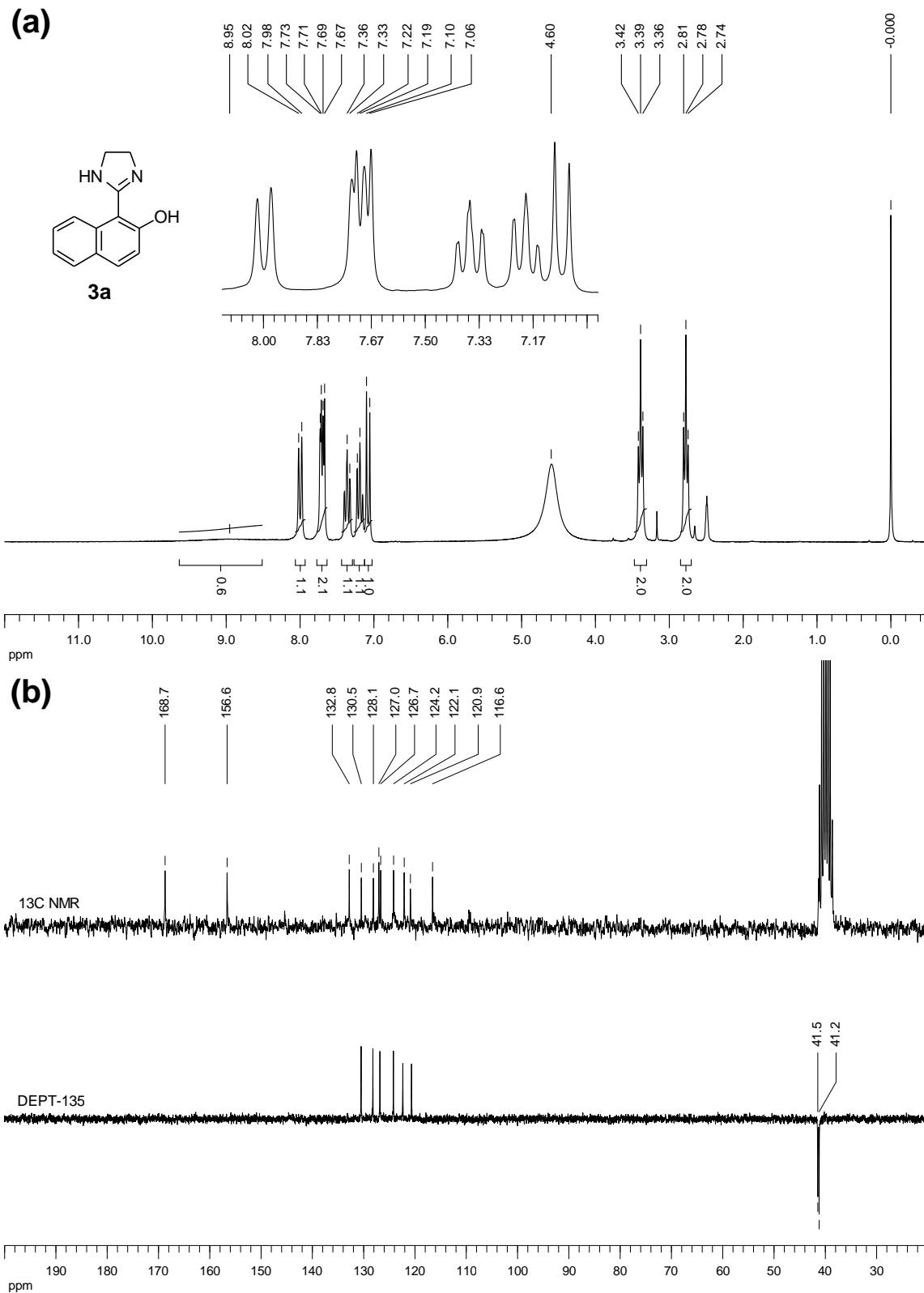


Fig. S4. NMR spectra for 1-(4,5-dihydro-1*H*-imidazol-2-yl)naphthalen-2-ol in DMSO-d6 (**3a**): (a) ¹H NMR spectrum at 200 MHz; (b) ¹³C NMR (top) and DEPT-135 (bottom) spectra at 50 MHz.

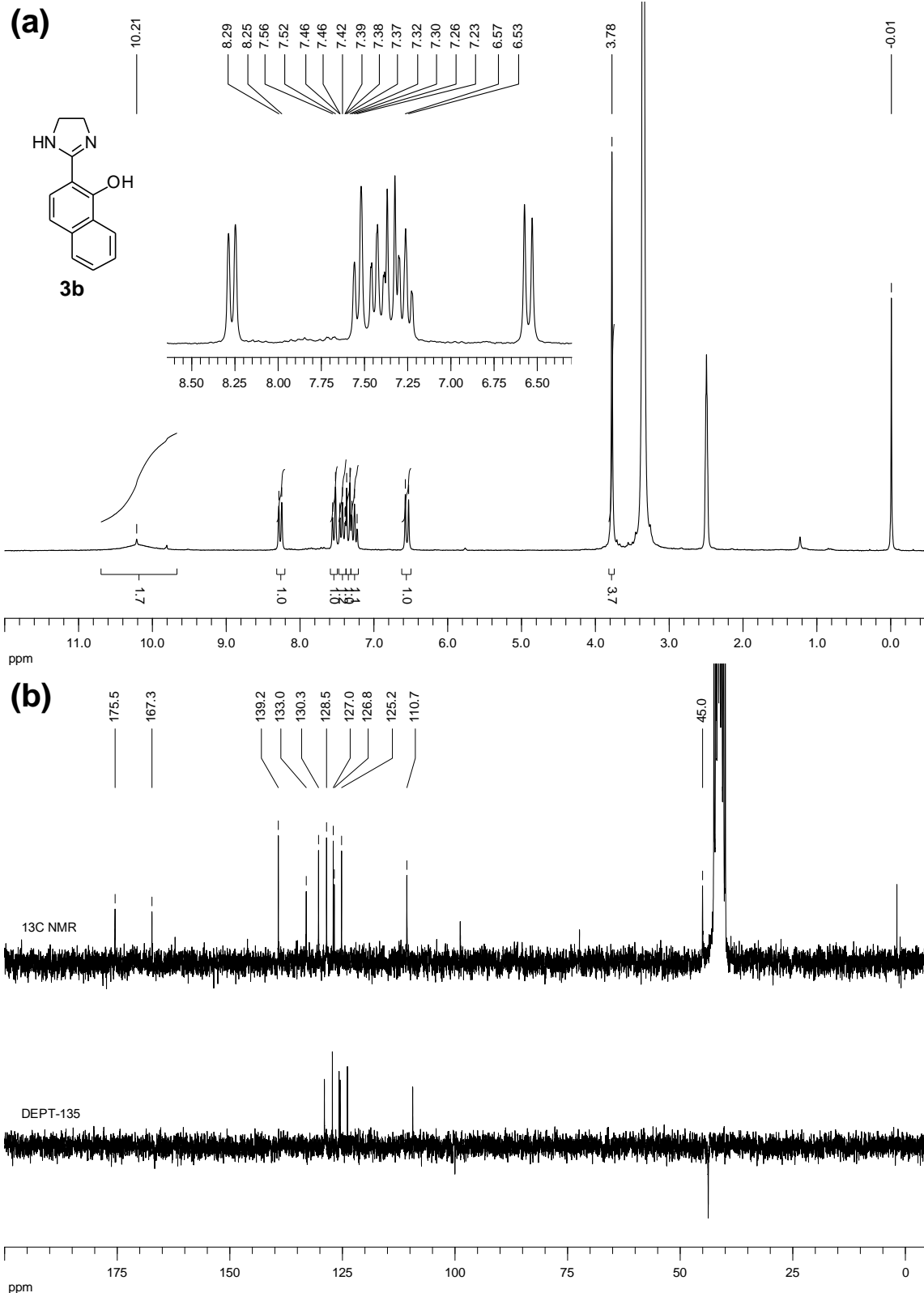


Fig. S5. NMR spectra for 2-(4,5-dihydro-1*H*-imidazol-2-yl)naphthalen-1-ol in DMSO-d₆ (**3b**): **(a)** ¹H NMR spectrum at 200 MHz; **(b)** ¹³C NMR (top) and DEPT-135 (bottom) spectra at 50 MHz.

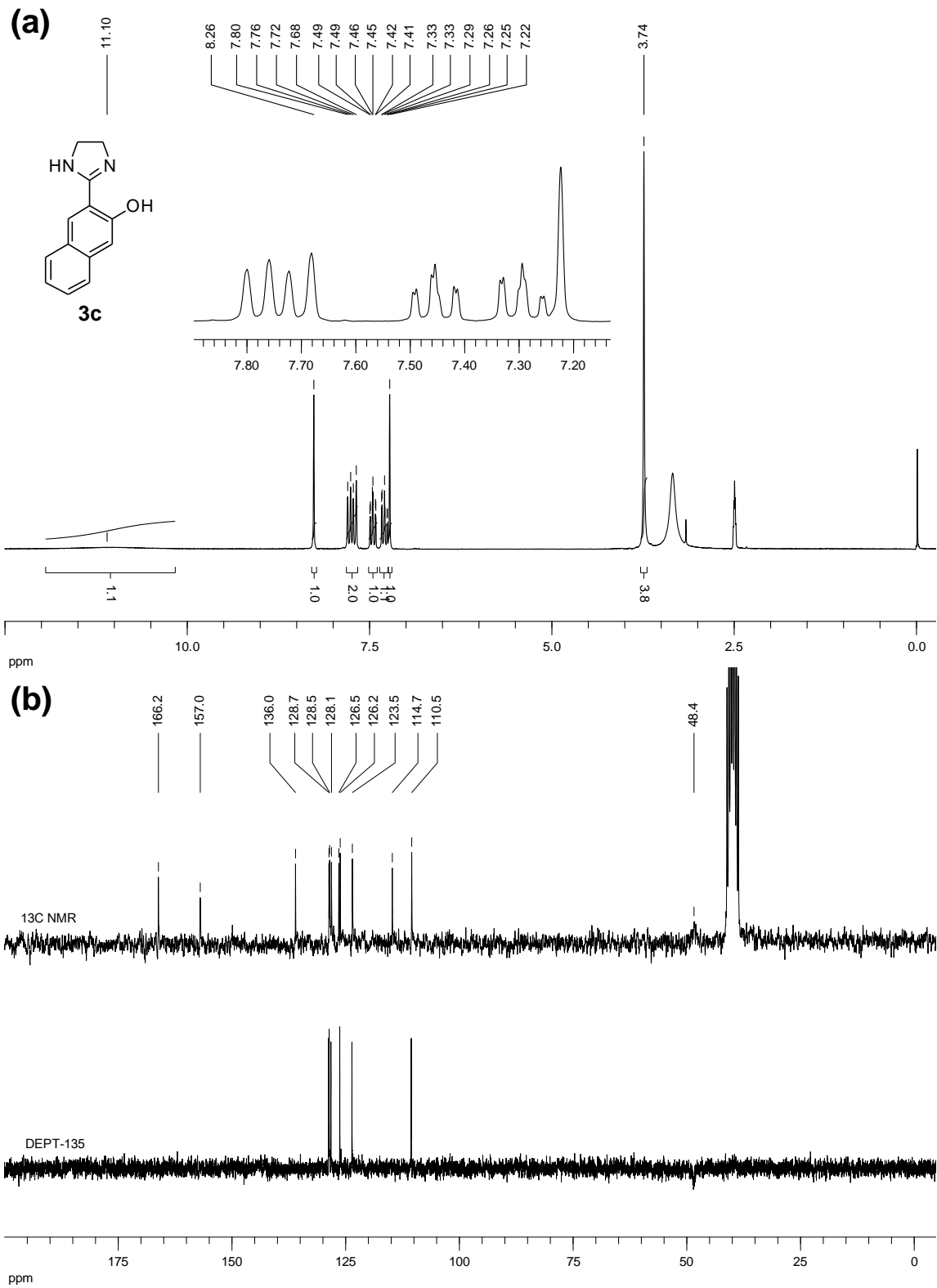


Fig. S6. NMR spectra for 3-(4,5-dihydro-1*H*-imidazol-2-yl)naphthalen-2-ol in DMSO-d₆ (**3c**): **(a)** ¹H NMR spectrum at 200 MHz; **(b)** ¹³C NMR (top) and DEPT-135 (bottom) spectra at 50 MHz.

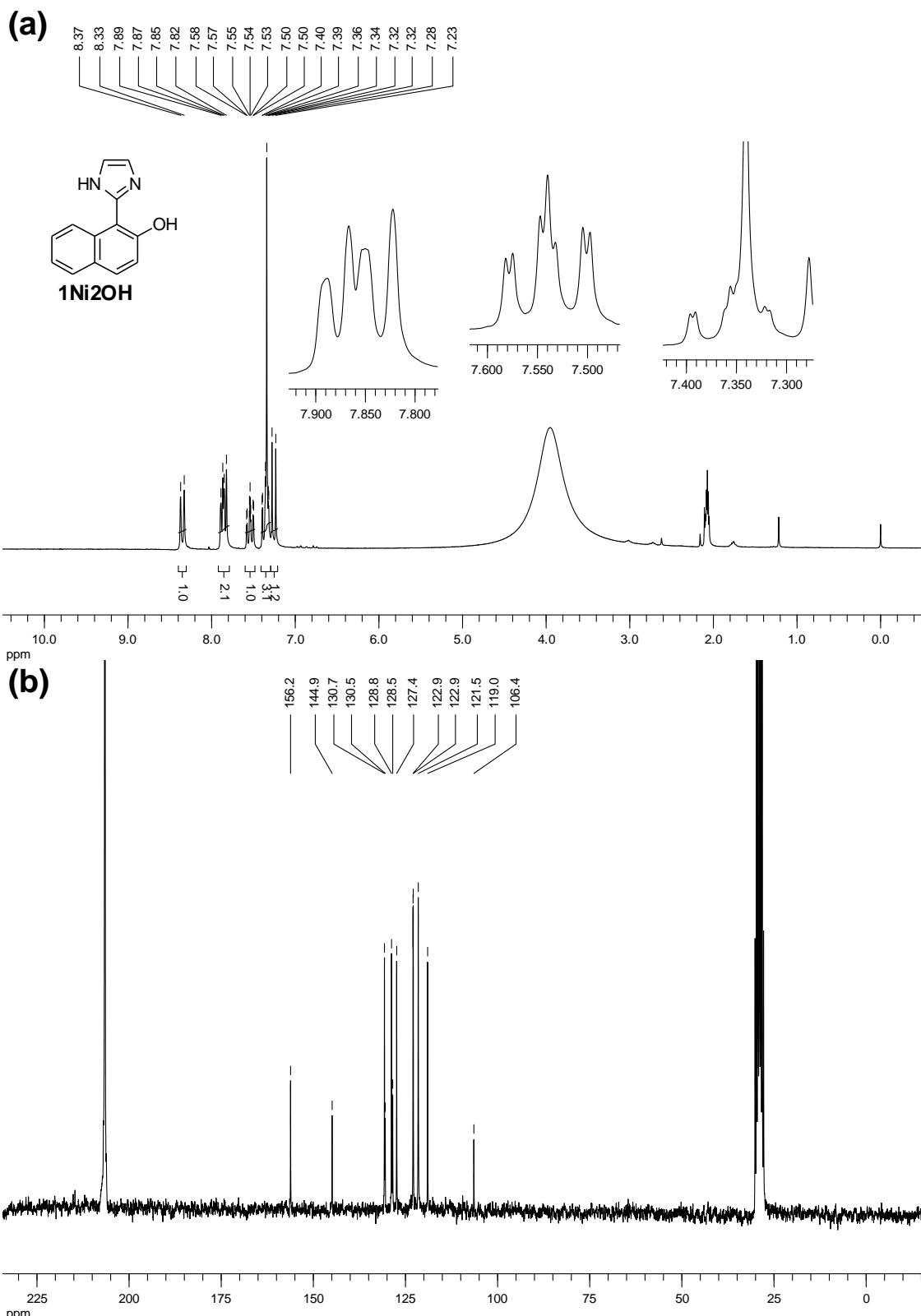


Fig. S7. NMR spectra for 1-(1*H*-imidazol-2-yl)naphthalen-2-ol (1NI2OH) in $(CD_3)_2CO$: **(a)** 1H NMR spectrum at 200 MHz; **(b)** ^{13}C NMR spectrum at 50 MHz.

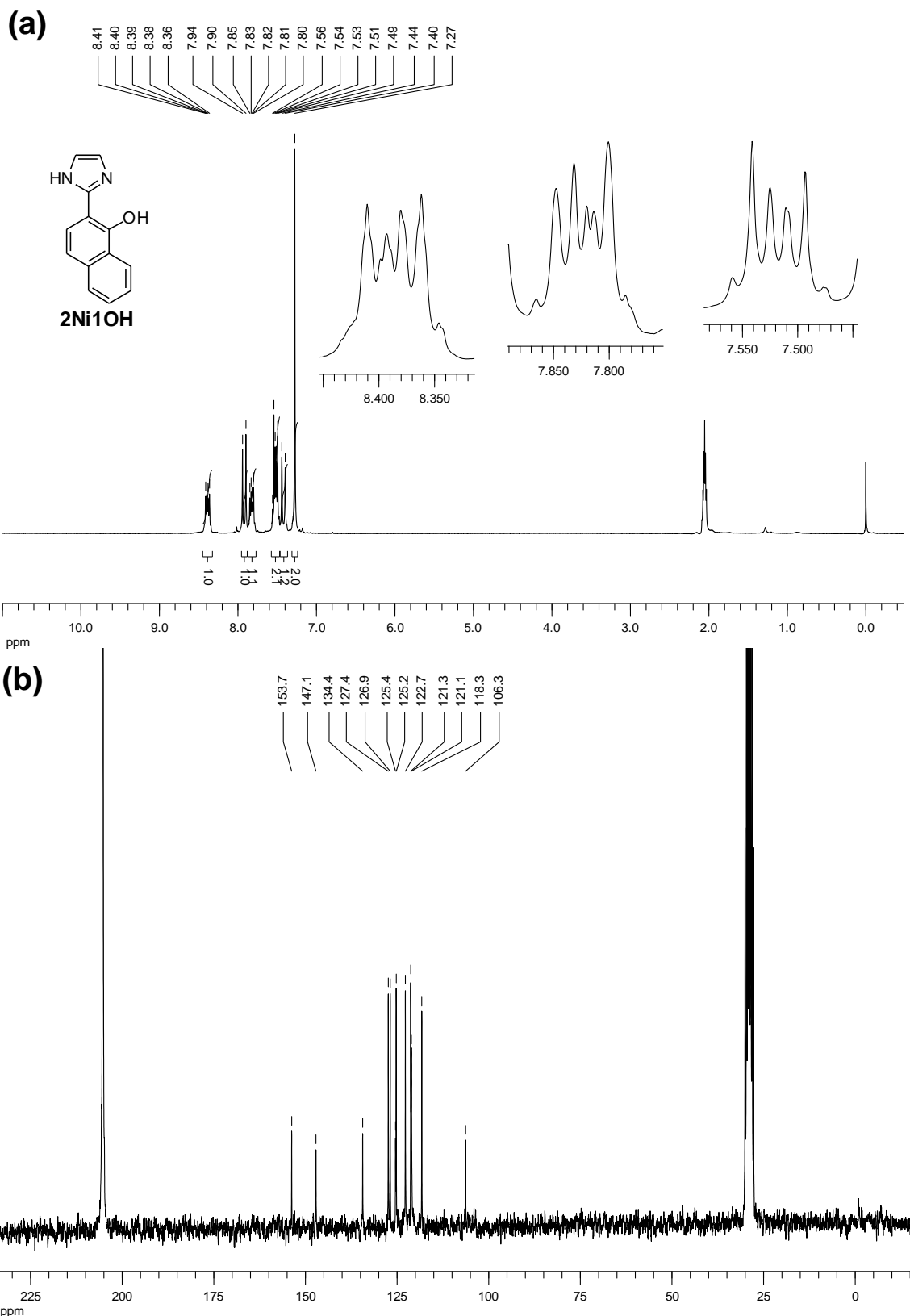


Fig. S8. NMR spectra for 2-(1*H*-imidazol-2-yl)naphthalen-1-ol (2Ni1OH) in ($\text{CD}_3\text{)}_2\text{CO}$: **(a)** ^1H NMR spectrum at 200 MHz; **(b)** ^{13}C NMR spectrum at 50 MHz.

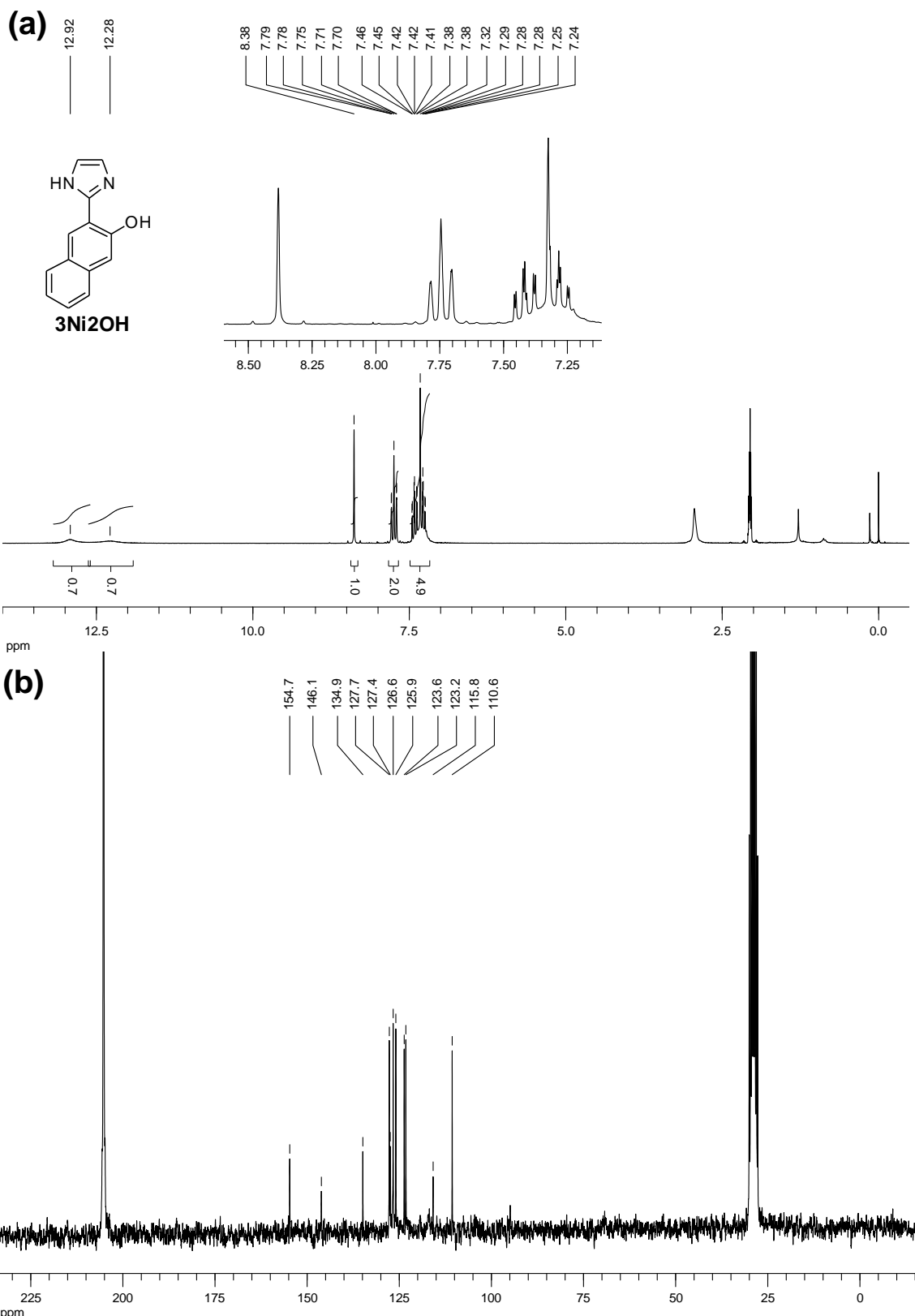


Fig. S9. NMR spectra for 3-(1*H*-imidazol-2-yl)naphthalen-2-ol (3NI2OH) in $(CD_3)_2CO$: **(a)** 1H NMR spectrum at 200 MHz; **(b)** ^{13}C NMR spectrum at 50 MHz.

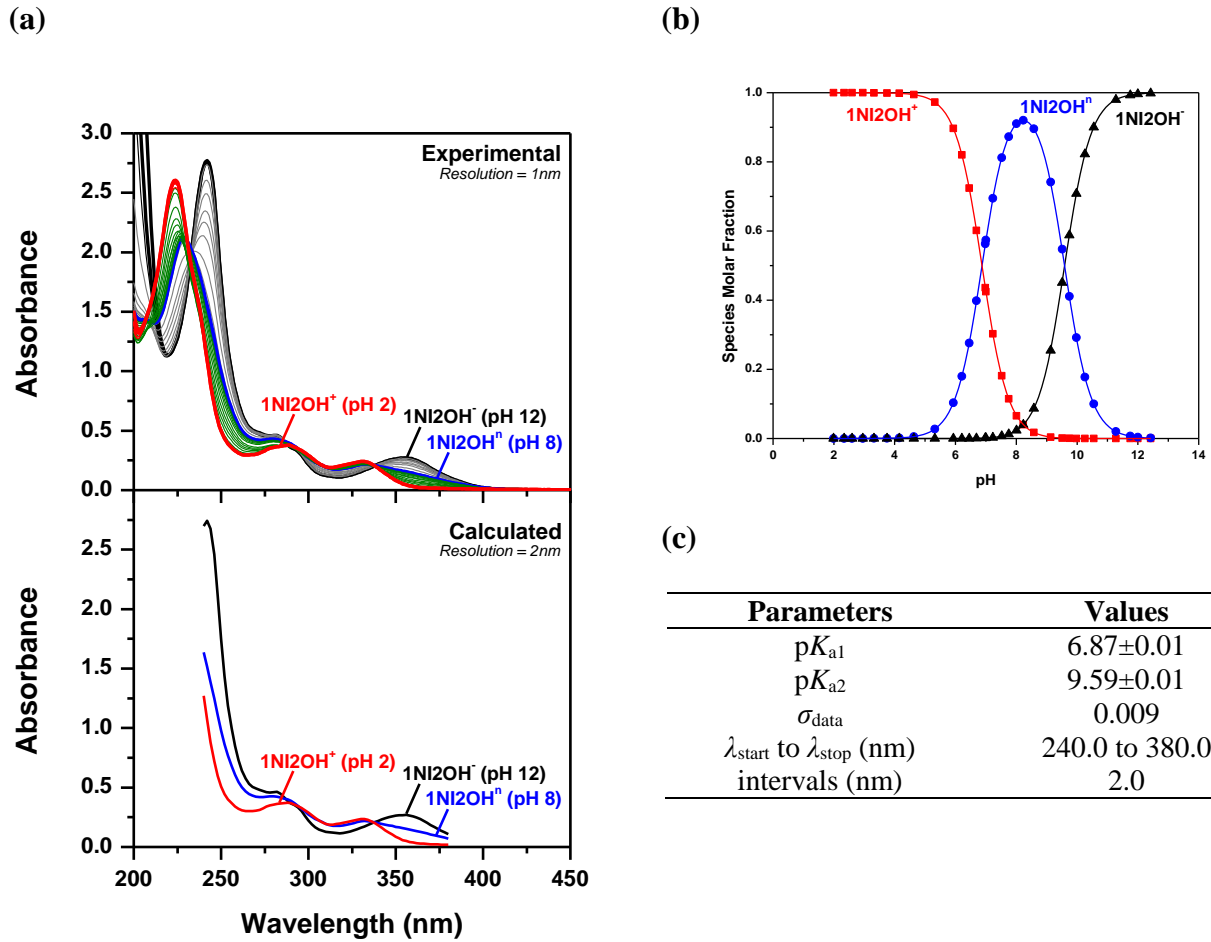


Fig. S10. Spectrophotometric, analytical and statistical data for the pH-titration of 1-(IH-imidazol-2-yl)naphthalen-2-ol (1NI2OH, 5.96×10^{-5} M) in aqueous 0.1 M KCl at 25 °C: (a) Experimental UV-Vis spectra and calculated spectra obtained by the software SQUAD using the molar absorptivities and the molar fractions for each species at the indicated pH; (b) Speciation diagram; (c) Calculated pK_a values obtained by the software SQUAD, standard deviation in the absorbance data (σ_{data}) and some other parameters used in the calculations. The spectra for the cationic, neutral and anionic species are shown in red, blue and black, respectively. The spectra shown in olive green (pH 3.0-7.8) represent the deprotonation of the cationic to the neutral species and the spectra in gray (pH 8.6-11.8) are for the deprotonation of the neutral to the anionic species.

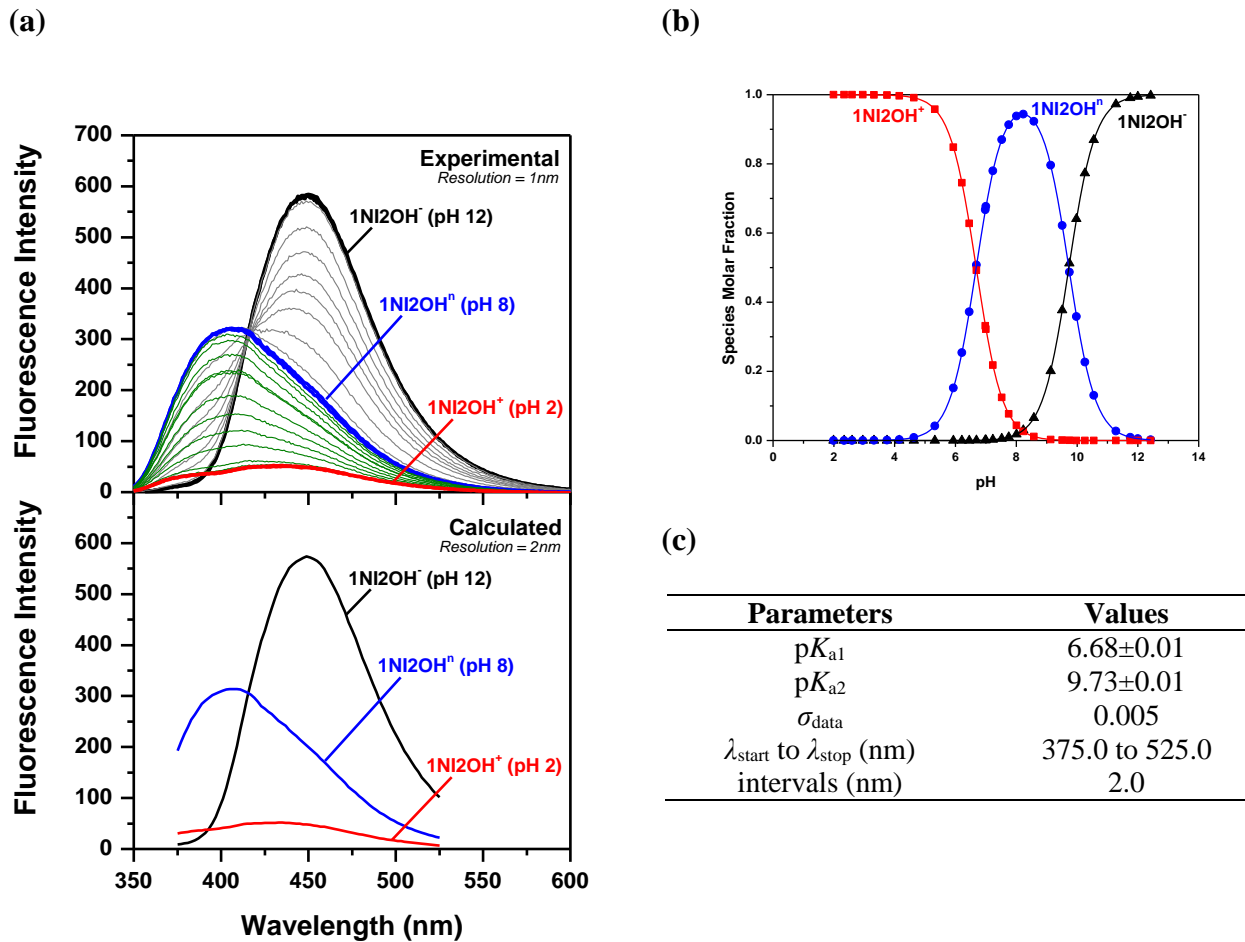


Fig. S11. Spectrofluorimetric, analytical and statistical data for the pH-titration of 1-(*IH*-imidazol-2-yl)naphthalen-2-ol (1NI2OH, 5.96×10^{-5} M) in aqueous 0.1 M KCl at 25 °C: (a) Experimental emission fluorescence spectra and calculated spectra obtained by the software SQUAD using the fluorescence contribution of each species at the indicated pH; (b) Speciation diagram; (c) Calculated pK_a values obtained by the software SQUAD, standard deviation in the fluorescence intensity data (σ_{data}) and some other parameters used in the calculations. The excitation wavelength was 330 nm using the following parameters: excitation slit of 10 nm; emission slit of 2.5 nm; and averaging time of 0.1 s. The spectra for the cationic, neutral and anionic species are shown in red, blue and black, respectively. The spectra shown in olive green (pH 3.0-7.8) represent the deprotonation of the cationic to the neutral species and the spectra in gray (pH 8.6-11.8) are for the deprotonation of the neutral to the anionic species.

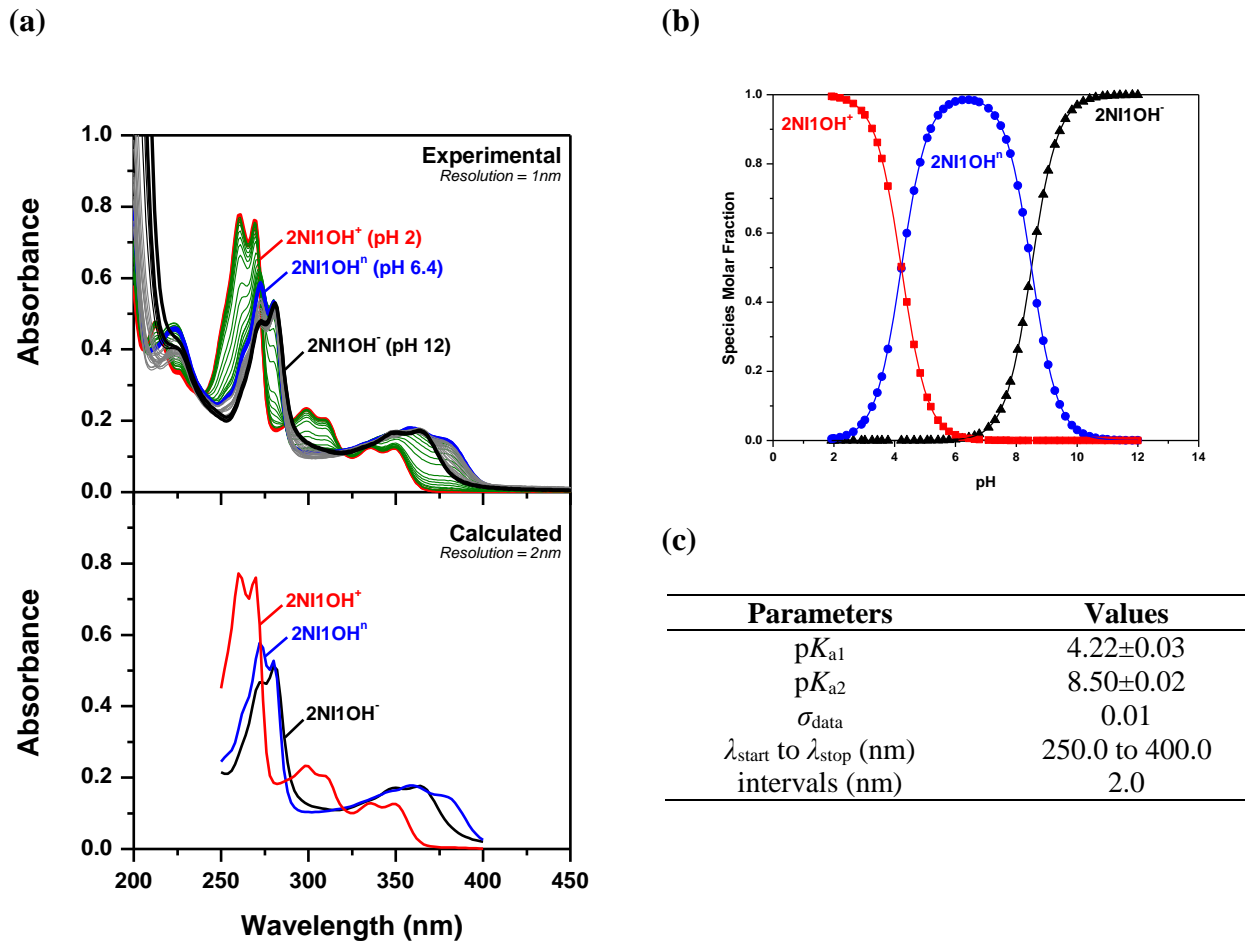


Fig. S12. Spectrophotometric, analytical and statistical data for the pH-titration of 2-(1*H*-imidazol-2-yl)naphthalen-1-ol (2NI1OH, 2.00×10^{-5} M) in aqueous 0.1 M KCl at 25 °C: (a) Experimental UV-Vis spectra and calculated spectra obtained by the software SQUAD using the molar absorptivities and the molar fractions for each species at the indicated pH; (b) Speciation diagram; (c) Calculated pK_a values obtained by the software SQUAD, standard deviation in the absorbance data (σ_{data}) and some other parameters used in the calculations. The spectra for the cationic, neutral and anionic species are shown in red, blue and black, respectively. The spectra shown in olive green (pH 2.4-5.8) represent the deprotonation of the cationic to the neutral species and the spectra in gray (pH 7.1-10.4) are for the deprotonation of the neutral to the anionic species.

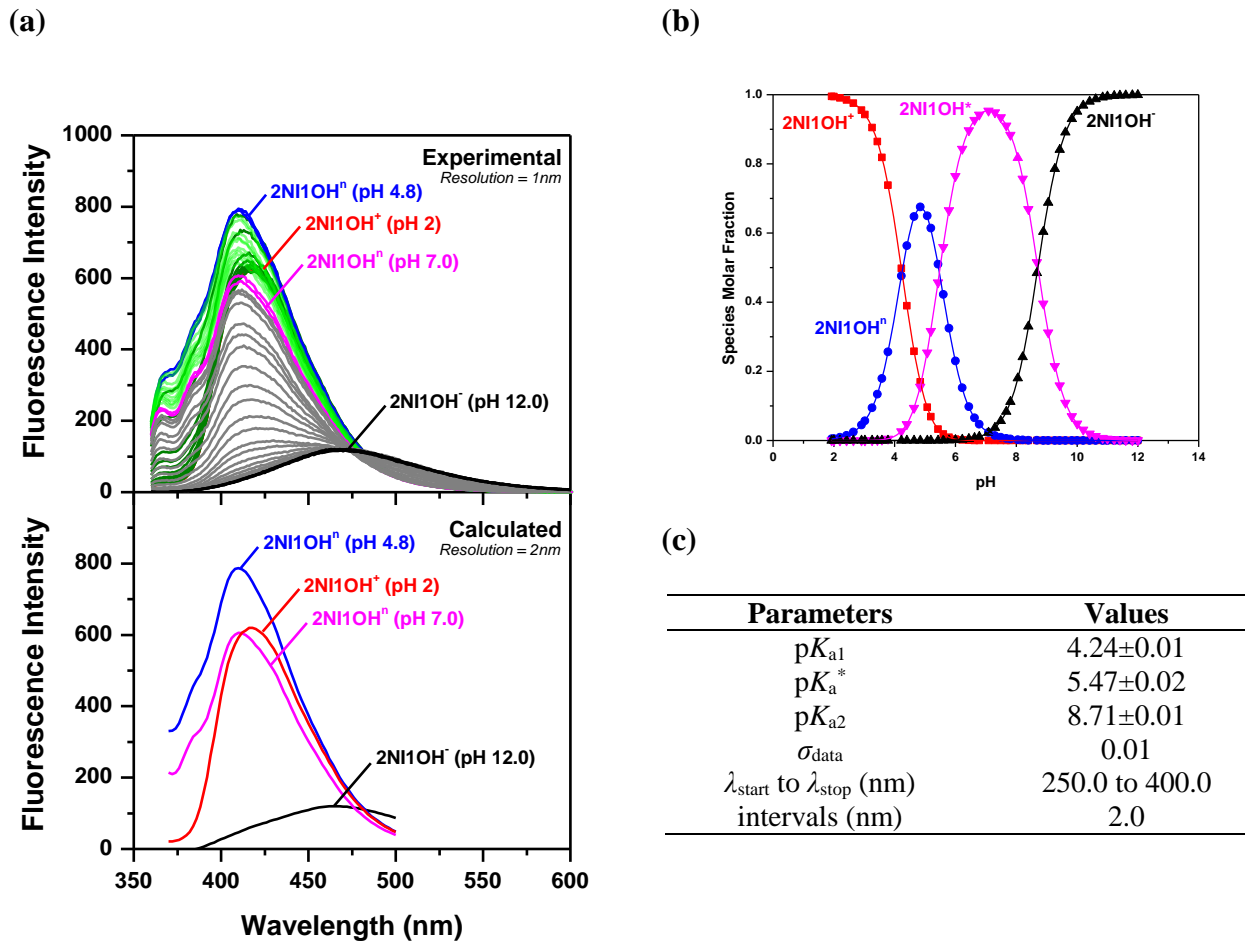


Fig. S13. Spectrofluorimetric, analytical and statistical data for the pH-titration of 2-(1*H*-imidazol-2-yl)naphthalen-1-ol (2NI1OH, 2.00×10^{-5} M) in aqueous 0.1 M KCl at 25 °C: (a) Experimental emission fluorescence spectra and calculated spectra obtained by the software SQUAD using the fluorescence contribution of each species at the indicated pH; (b) Speciation diagram; (c) Calculated pK_a values obtained by the software SQUAD, standard deviation in the fluorescence intensity data (σ_{data}) and some other parameters used in the calculations. The excitation wavelength was 350 nm using the following parameters: excitation slit of 10 nm; emission slit of 2.5 nm; and averaging time of 0.1 s. The spectra for the cationic, neutral and anionic species are shown in red, blue and black, respectively. The spectrum for 2NI1OH⁺ perturbed by the excited state is shown in magenta. The spectra shown in olive green (pH 2.4-5.8) represent the deprotonation of the cationic to the neutral species and the spectra in gray (pH 7.1-10.4) are for the deprotonation of the neutral to the anionic species. The spectra in light green represent the effect at the excited state between pH 4.8 and 7.0.

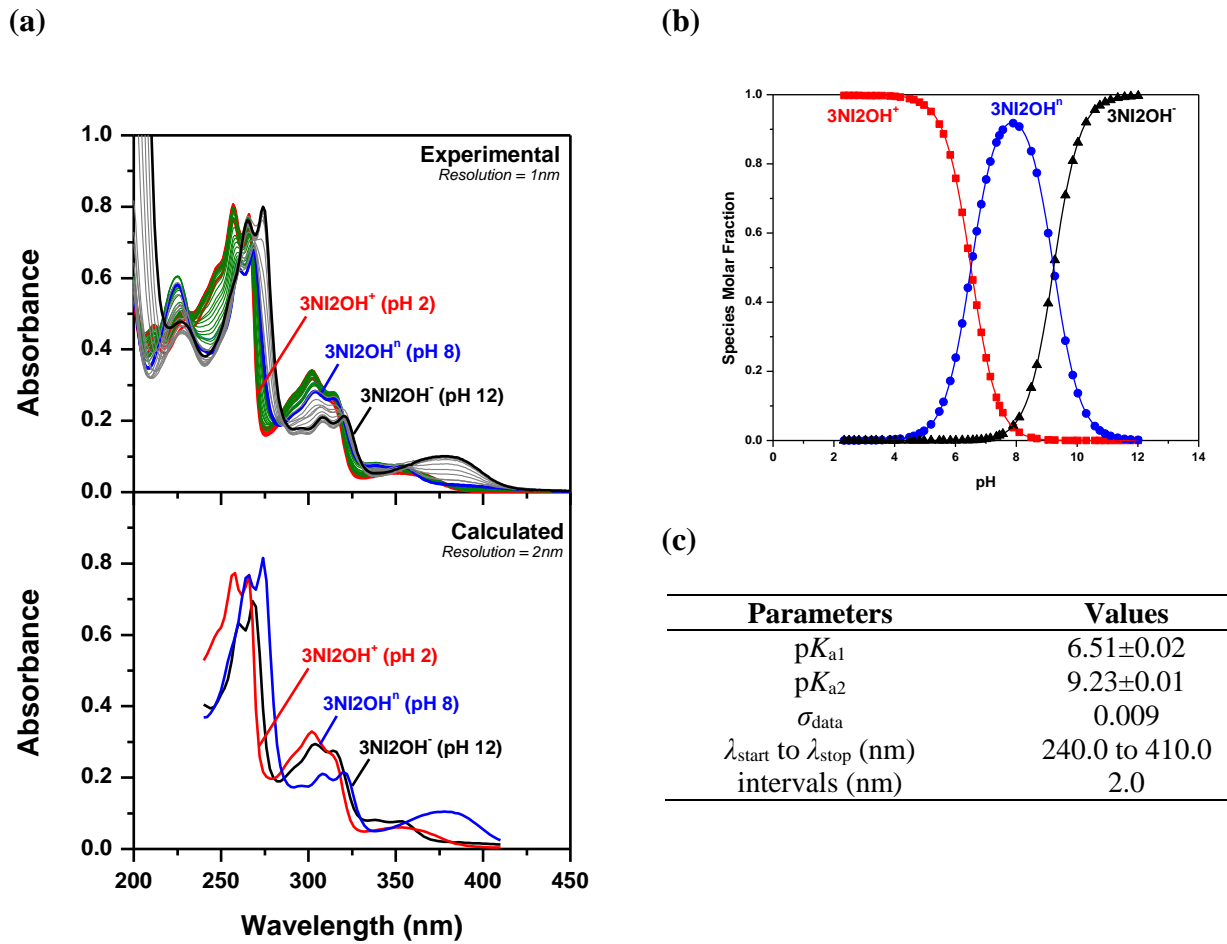


Fig. S14. Spectrophotometric, analytical and statistical data for the pH-titration of 3-(1*H*-imidazol-2-yl)naphthalen-2-ol (3NI2OH, 2.00×10^{-5} M) in aqueous 0.1 M KCl at 25 °C: (a) Experimental UV-Vis spectra and calculated spectra obtained by the software SQUAD using the molar absorptivities and the molar fractions for each species at the indicated pH; (b) Speciation diagram; (c) Calculated pK_a values obtained by the software SQUAD, standard deviation in the absorbance data (σ_{data}) and some other parameters used in the calculations. The spectra for the cationic, neutral and anionic species are shown in red, blue and black, respectively. The spectra shown in olive green (pH 4.2-7.6) represent the deprotonation of the cationic to the neutral species and the spectra in gray (pH 8.5-11.1) are for the deprotonation of the neutral to the anionic species.

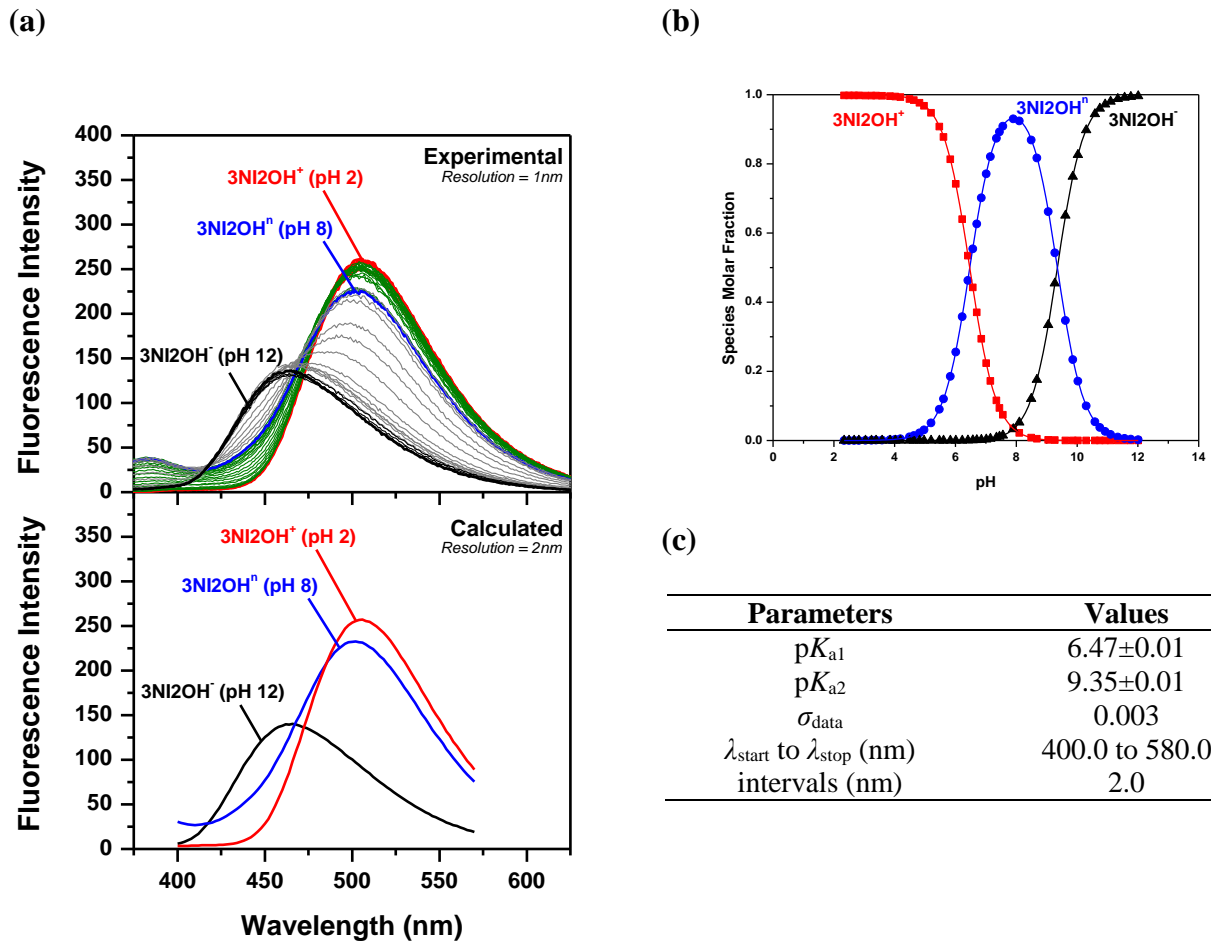
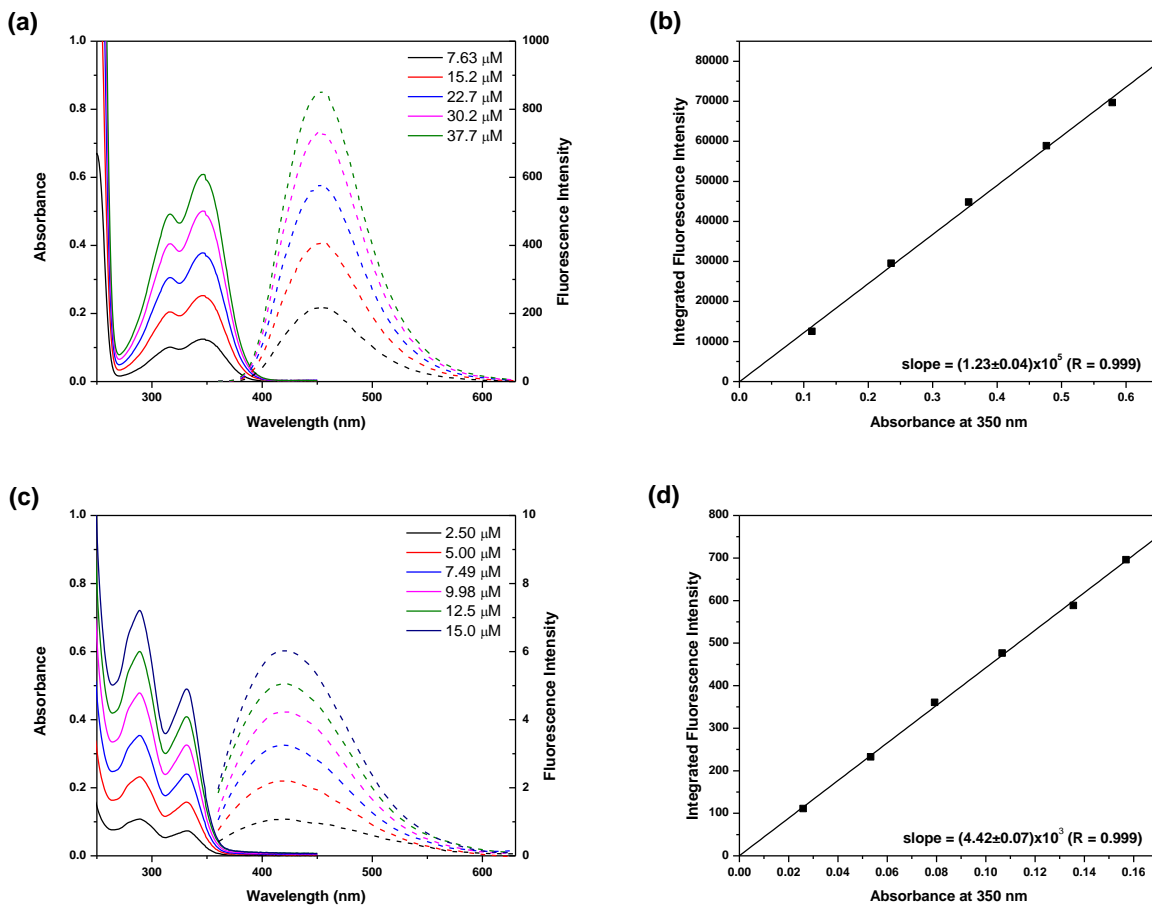
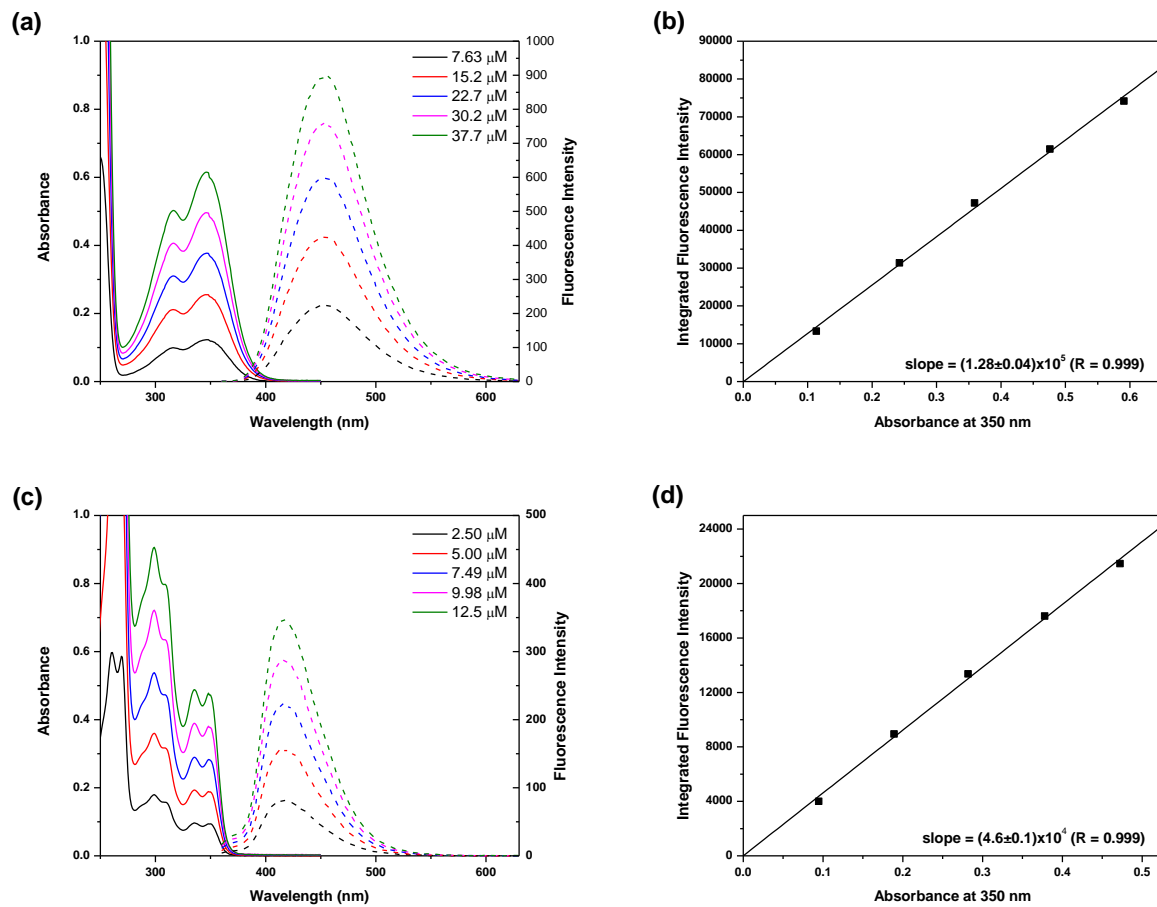


Fig. S15. Spectrofluorimetric, analytical and statistical data for the pH-titration of 3-(1*H*-imidazol-2-yl)naphthalen-2-ol (3NI2OH, 2.00×10^{-5} M) in aqueous 0.1 M KCl at 25 °C: (a) Experimental emission fluorescence spectra and calculated spectra obtained by the software SQUAD using the fluorescence contribution of each species at the indicated pH; (b) Speciation diagram; (c) Calculated pK_a values obtained by the software SQUAD, standard deviation in the fluorescence intensity data (σ_{data}) and some other parameters used in the calculations. The excitation wavelength was 350 nm using the following parameters: excitation slit of 10 nm; emission slit of 2.5 nm; and averaging time of 0.1 s. The spectra for the cationic, neutral and anionic species are shown in red, blue and black, respectively. The spectra shown in olive green (pH 4.2-7.6) represent the deprotonation of the cationic to the neutral species and the spectra in gray (pH 8.5-11.1) are for the deprotonation of the neutral to the anionic species.



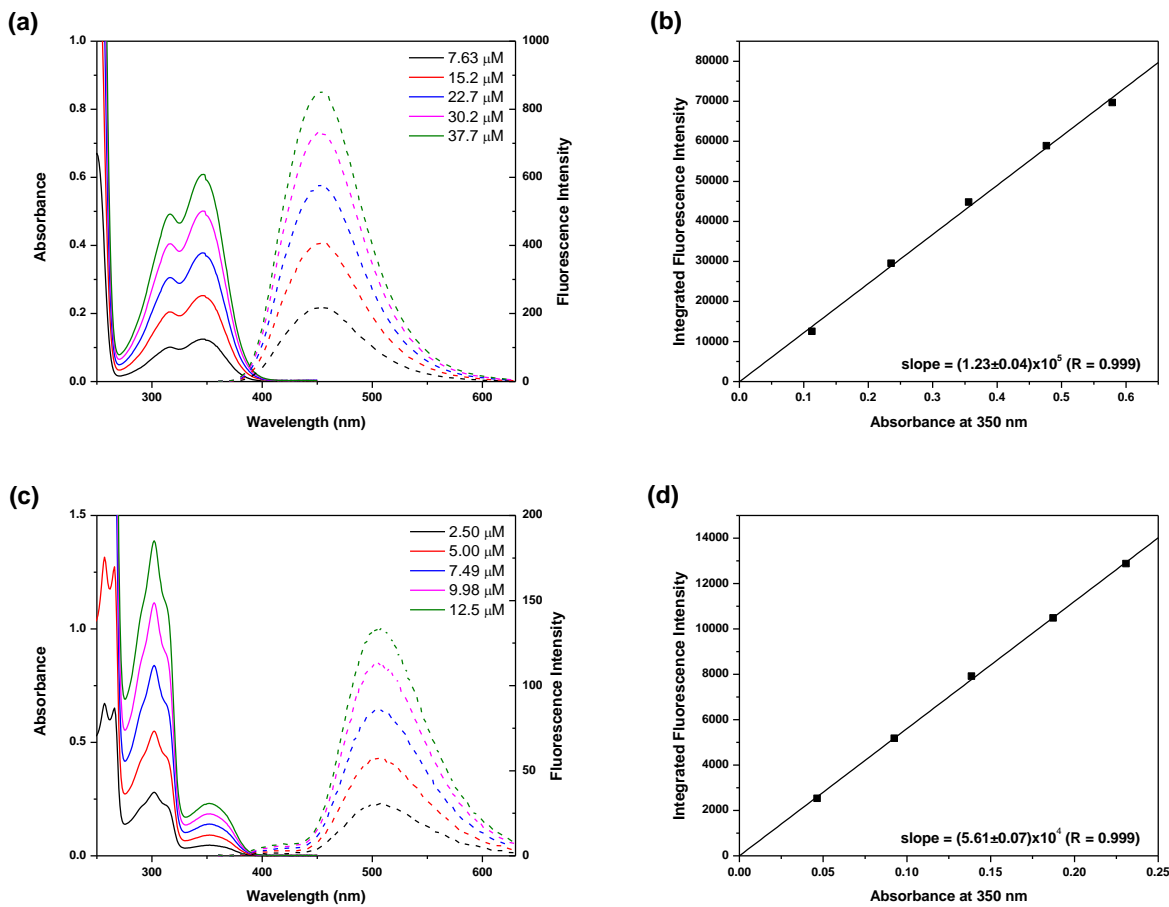
$$\Phi_{1\text{NI}2\text{OH}} = \Phi_{\text{QS}} \left(\frac{\text{slope}_{1\text{NI}2\text{OH}}}{\text{slope}_{\text{QS}}} \right) \left(\frac{\eta_{1\text{NI}2\text{OH}}^2}{\eta_{\text{QS}}^2} \right) = 0.546 \left[\frac{(4.42 \pm 0.07) \times 10^{-3}}{(1.23 \pm 0.04) \times 10^5} \right] = 0.0196 \pm 0.0007$$

Fig. S16. Determination of the quantum yield (Φ) for 1-(1*H*-imidazol-2-yl)naphthalen-2-ol (1NI2OH): (a) absorption (solid line) and emission (broken line) spectra for the standard sample, quinine sulfate (QS), in 0.1 M aqueous H₂SO₄ at 25 °C ($\Phi_{\text{QS}} = 0.546$)²; (b) integrated fluorescence intensity *vs* absorbance for QS; (c) absorption (solid line) and emission (broken line) spectra for 1NI2OH in 0.1 M aqueous H₂SO₄ at 25 °C; (d) integrated fluorescence intensity *vs* absorbance for 1NI2OH. The equation shown above was used to calculate the quantum yield for 1NI2OH. The slope was obtained from the plot of the integrated fluorescence intensity *vs* absorbance and η is the refractive index of the solvent. Cuvettes of 3 cm and 1 cm of pathlengths were used to acquire the absorption and emission spectra, respectively. Sample concentrations are shown in the graphs.



$$\Phi_{2\text{Ni1OH}} = \Phi_{\text{QS}} \left(\frac{\text{slope}_{2\text{Ni1OH}}}{\text{slope}_{\text{QS}}} \right) \left(\frac{\eta_{2\text{Ni1OH}}^2}{\eta_{\text{QS}}^2} \right) = 0.546 \left[\frac{(4.6 \pm 0.1) \times 10^4}{(1.28 \pm 0.04) \times 10^5} \right] = 0.196 \pm 0.007$$

Fig. S17. Determination of the quantum yield (Φ) for 2-(1*H*-imidazol-2-yl)naphthalen-1-ol (2NI1OH): (a) absorption (solid line) and emission (broken line) spectra for the standard sample, quinine sulfate (QS), in 0.1 M aqueous H₂SO₄ at 25 °C ($\Phi_{\text{QS}} = 0.546$)²; (b) integrated fluorescence intensity *vs* absorbance for QS; (c) absorption (solid line) and emission (broken line) spectra for 2NI1OH in 0.1 M aqueous H₂SO₄ at 25 °C; (d) integrated fluorescence intensity *vs* absorbance for 2NI1OH. The equation shown above was used to calculate the quantum yield for 2NI1OH. The slope was obtained from the plot of the integrated fluorescence intensity *vs* absorbance and η is the refractive index of the solvent. Cuvettes of 3 cm and 1 cm of pathlengths were used to acquire the absorption and emission spectra, respectively. Sample concentrations are shown in the graphs.



$$\Phi_{3\text{Ni}2\text{OH}} = \Phi_{\text{QS}} \left(\frac{\text{slope}_{3\text{Ni}2\text{OH}}}{\text{slope}_{\text{QS}}} \right) \left(\frac{\eta_{3\text{Ni}2\text{OH}}^2}{\eta_{\text{QS}}^2} \right) = 0.546 \left[\frac{(5.61 \pm 0.07) \times 10^4}{(1.23 \pm 0.04) \times 10^5} \right] = 0.249 \pm 0.009$$

Fig. S18. Determination of the quantum yield (Φ) for 3-(1*H*-imidazol-2-yl)naphthalen-2-ol (3NI2OH): (a) absorption (solid line) and emission (broken line) spectra for the standard sample, quinine sulfate (QS), in 0.1 M aqueous H₂SO₄ at 25 °C ($\Phi_{\text{QS}} = 0.546$)²; (b) integrated fluorescence intensity *vs* absorbance for QS; (c) absorption (solid line) and emission (broken line) spectra for 3NI2OH in 0.1 M aqueous H₂SO₄ at 25 °C; (d) integrated fluorescence intensity *vs* absorbance for 3NI2OH. The equation shown above was used to calculate the quantum yield for 3NI2OH. The slope was obtained from the plot of the integrated fluorescence intensity *vs* absorbance and η is the refractive index of the solvent. Cuvettes of 3 cm and 1 cm of pathlengths were used to acquire the absorption and emission spectra, respectively. Sample concentrations are shown in the graphs.

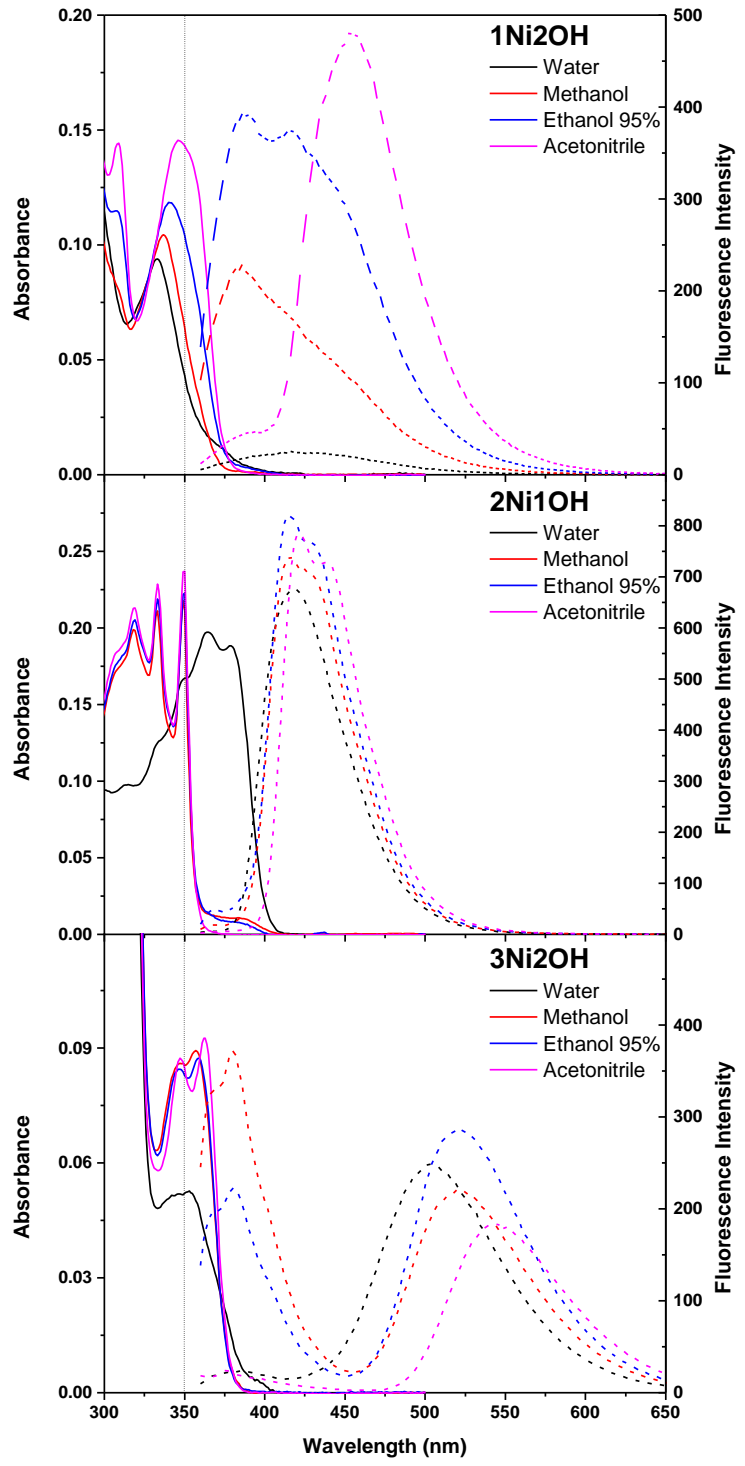
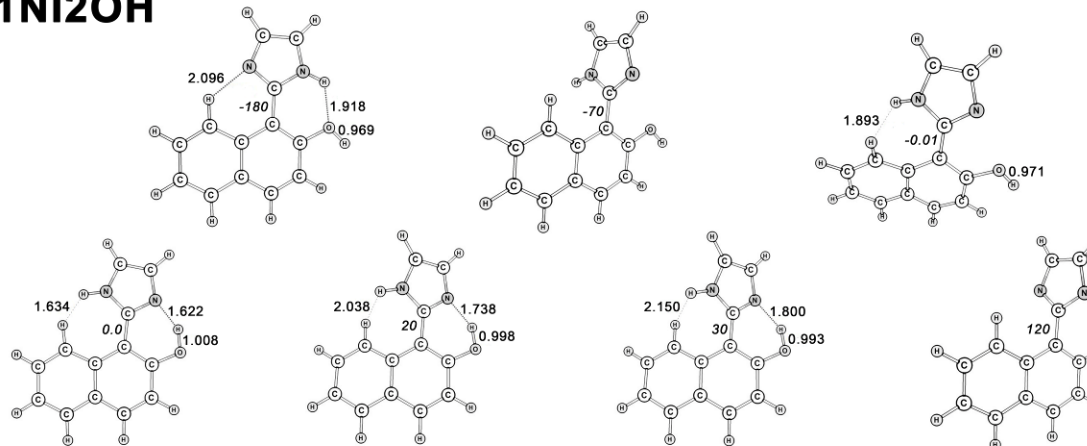
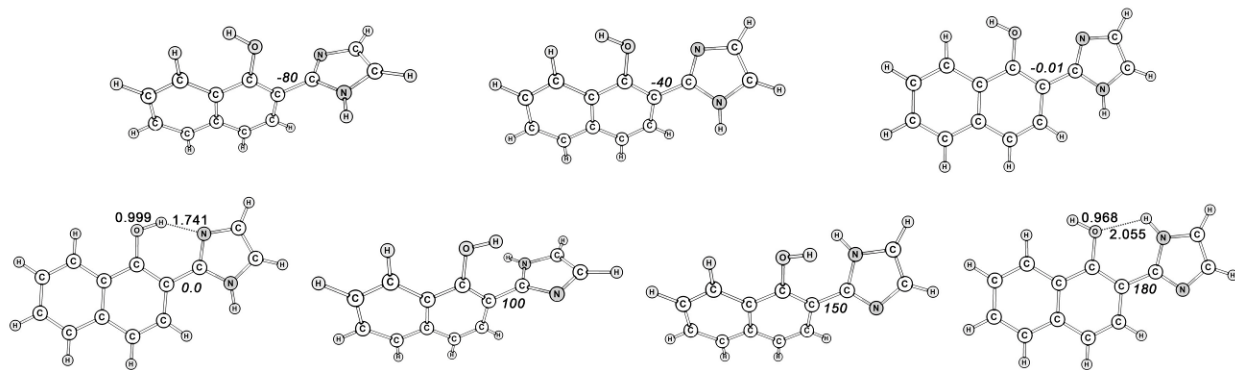


Fig. S19. Absorption (solid line) and emission (broken line) spectra for 1-(1*H*-imidazol-2-yl)naphthalen-2-ol (**1Ni2OH**, 1×10^{-5} M), 2-(1*H*-imidazol-2-yl)naphthalen-1-ol (**2Ni1OH**, 1×10^{-5} M) and 3-(1*H*-imidazol-2-yl)naphthalen-2-ol (**3Ni2OH**, 2×10^{-5} M) in different solvents at 25 °C. The excitation for the emission spectra was performed at 350 nm (dotted line). The emission spectra were uncorrected for absorption effects.

1NI2OH



2NI1OH



3NI2OH

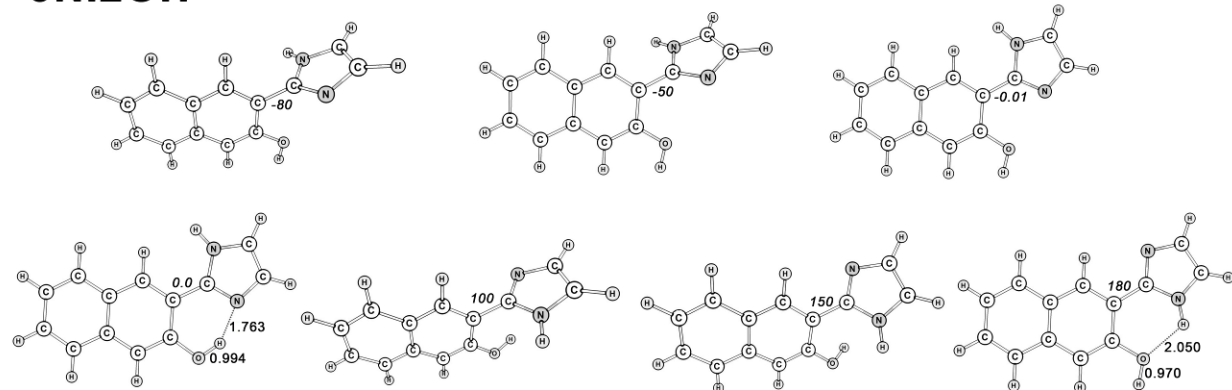


Fig. S20. Selected structures along the Potential Energy Surface in the ground state for the rotation around the interannular bond between the naphthal and the imidazole ring of 1NI2OH, 2NI1OH, and 3NI2OH. Torsion angles for interannular bonds are shown in degree and italic. Bond lengths are in angstroms.

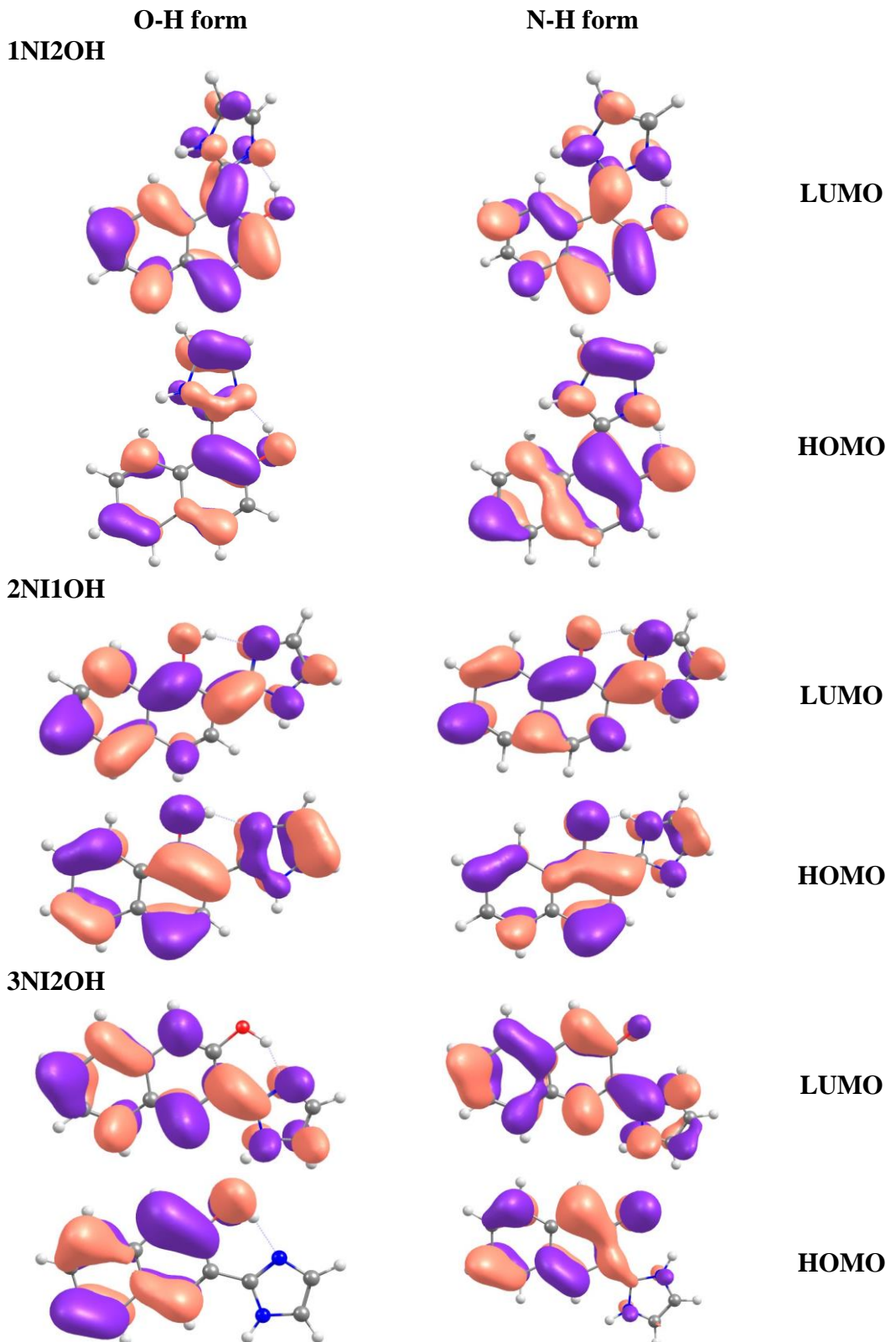


Fig. S21. HOMO and LUMO orbital diagrams for optimized structures of 1NI2OH, 2NI1OH, and 3NI2OH in Fig. 4.

Table S1. Cartesian coordinates for the S₀-N_{syn} and S₀-PT forms of 1NI2OH shown in Fig. 4.

	S ₀ -N _{syn}			S ₀ -PT		
	x	y	z	x	y	z
N	0.001368	0.009604	-0.031982	0.009211	-0.008476	0.007187
C	1.369311	-0.003985	-0.000265	1.375275	0.001222	0.004025
N	1.819808	1.247347	0.040951	1.725875	1.309274	-0.000179
C	0.722895	2.070098	0.035600	0.606015	2.109173	0.052729
C	-0.418401	1.322701	-0.006545	-0.474106	1.294291	0.057224
C	2.220530	-1.182150	0.120687	2.319831	-1.058842	0.092234
C	1.812162	-2.501769	-0.271910	1.969544	-2.454899	-0.020012
C	2.603888	-3.625767	0.123102	2.933071	-3.439468	0.357858
C	3.813405	-3.399840	0.831060	4.240531	-3.016309	0.758076
C	4.248079	-2.135544	1.095791	4.599739	-1.712966	0.771904
C	3.474233	-1.010106	0.722759	3.672925	-0.657528	0.420081
C	2.196537	-4.931868	-0.233766	2.609241	-4.806483	0.301565
C	1.071079	-5.147840	-0.991124	1.377983	-5.239128	-0.143762
C	0.324988	-4.043405	-1.441230	0.449728	-4.288844	-0.583481
C	0.681880	-2.762347	-1.089973	0.739773	-2.938716	-0.530011
O	3.996878	0.190811	1.009790	4.063798	0.549018	0.444747
H	2.806312	-5.766780	0.093257	3.359627	-5.525698	0.611504
H	0.774383	-6.151140	-1.269552	1.140617	-6.294862	-0.179265
H	-0.528702	-4.200984	-2.089193	-0.498883	-4.613836	-0.994208
H	0.125858	-1.939536	-1.516018	0.024930	-2.258830	-0.971822
H	5.183182	-1.949746	1.607393	5.596309	-1.398018	1.053598
H	4.401604	-4.253821	1.145711	4.956771	-3.781093	1.039992
H	-0.591089	-0.801551	0.022725	-0.541887	-0.839899	0.131644
H	-1.459314	1.592963	-0.030196	-1.526126	1.513302	0.072050
H	0.821864	3.142465	0.060077	0.669061	3.182323	0.067372
H	3.371278	0.892119	0.680729	2.755110	1.470544	0.132445

Table S2. Cartesian coordinates for the S₁-N_{syn} and S₁-PT forms of 1NI2OH shown in Fig. 4.

	S ₁ -N _{syn}			S ₁ -PT		
	x	y	z	x	y	z
N	-0.001819	0.009614	-0.007791	0.008844	-0.010032	0.020531
C	1.377124	-0.006598	0.002772	1.382491	0.001958	0.000870
N	1.822408	1.272223	0.009625	1.726817	1.323208	-0.015884
C	0.736216	2.072086	0.018350	0.605765	2.110060	0.109739
C	-0.419665	1.304101	0.017125	-0.471443	1.284542	0.128405
C	2.204580	-1.160491	0.081605	2.275853	-1.084214	0.102705
C	1.675317	-2.512027	-0.061721	1.881693	-2.453982	-0.152410
C	2.459149	-3.574036	0.491725	2.704288	-3.493083	0.421091
C	3.769534	-3.304185	0.945897	3.958745	-3.161373	0.986218
C	4.357621	-2.048300	0.909737	4.467687	-1.869521	0.982973
C	3.578779	-0.962194	0.493495	3.653279	-0.787815	0.560789
C	1.919064	-4.896336	0.508672	2.231741	-4.824116	0.346461
C	0.687365	-5.166841	-0.088353	1.065697	-5.144785	-0.338304
C	-0.032447	-4.159827	-0.708960	0.324481	-4.152624	-0.983592
C	0.460628	-2.823610	-0.692224	0.743622	-2.817369	-0.885217
O	4.132179	0.244379	0.536819	4.050494	0.419390	0.563049
H	2.490433	-5.689317	0.974596	2.809940	-5.608004	0.821505
H	0.301235	-6.179928	-0.076868	0.742959	-6.178188	-0.386824
H	-0.974227	-4.375863	-1.196165	-0.559391	-4.405036	-1.553756
H	-0.041852	-2.088749	-1.307130	0.196244	-2.062450	-1.436225
H	5.381430	-1.876002	1.206974	5.453903	-1.638786	1.358845
H	4.357977	-4.143445	1.302419	4.563420	-3.969480	1.382333
H	-0.565827	-0.828316	0.061689	-0.523532	-0.856753	0.149689
H	-1.460182	1.579322	0.015671	-1.523071	1.504209	0.167144
H	0.816605	3.147096	0.016145	0.656676	3.183924	0.132949
H	3.447615	0.934109	0.294438	2.728518	1.516910	0.141142

Table S3. Cartesian coordinates for the S₀-N_{syn} and S₀-PT forms of 2NI1OH shown in Fig. 4.

	S ₀ -N _{syn}			S ₀ -PT		
	x	y	z	x	y	z
N	-0.000669	0.006489	-0.000211	0.008828	-0.005889	0.000044
C	1.366308	-0.011509	-0.000130	1.373034	0.008329	-0.000195
N	1.828118	1.234278	0.000540	1.725196	1.314070	-0.000097
C	0.735532	2.064534	0.000795	0.602371	2.115220	0.000211
C	-0.411501	1.324580	0.000267	-0.476821	1.298622	0.000282
C	2.198380	-1.201737	-0.000366	2.292829	-1.065612	-0.000400
C	3.590474	-1.066727	-0.000481	3.696952	-0.728712	-0.000850
C	4.426078	-2.225948	-0.000230	4.633454	-1.857715	-0.000872
C	3.826592	-3.518181	-0.000063	4.159751	-3.195970	-0.000583
C	2.410339	-3.627340	-0.000133	2.750607	-3.456128	-0.000229
C	1.634209	-2.504957	-0.000272	1.864885	-2.426145	-0.000144
C	5.836961	-2.113959	-0.000169	6.017106	-1.610847	-0.001224
C	6.625362	-3.239523	0.000064	6.920771	-2.653543	-0.001289
C	6.036322	-4.520470	0.000227	6.458214	-3.979389	-0.001010
C	4.669644	-4.654351	0.000146	5.105424	-4.243557	-0.000663
O	4.203973	0.125605	-0.001082	4.116760	0.465060	-0.001168
H	6.278563	-1.126772	-0.000276	6.347338	-0.580176	-0.001440
H	7.704437	-3.144055	0.000129	7.985157	-2.451516	-0.001554
H	6.667085	-5.400865	0.000406	7.167601	-4.798451	-0.001069
H	4.215359	-5.638347	0.000260	4.749954	-5.267792	-0.000447
H	1.953799	-4.609394	-0.000013	2.403732	-4.482037	-0.000003
H	0.555782	-2.619678	-0.000172	0.802984	-2.654418	0.000168
H	-0.606145	-0.796061	-0.000593	-0.551914	-0.839583	0.000086
H	-1.450776	1.602123	0.000270	-1.528694	1.518551	0.000524
H	0.839963	3.136625	0.001345	0.661954	3.188487	0.000370
H	3.507941	0.838116	-0.001732	2.754157	1.481580	-0.000207

Table S4. Cartesian coordinates for the S₁-N_{syn} and S₁-PT forms of 2NI1OH shown in Fig. 4.

	S ₁ -N _{syn}			S ₁ -PT		
	x	y	z	x	y	z
N	-0.004896	0.008701	0.000350	0.010208	-0.005547	-0.000058
C	1.378106	-0.008428	-0.000157	1.390152	0.010068	0.000085
N	1.828592	1.266223	-0.000806	1.735259	1.329164	0.000126
C	0.742719	2.070687	-0.000633	0.617746	2.120406	-0.000049
C	-0.415404	1.316321	0.000121	-0.468542	1.303934	-0.000160
C	2.187544	-1.171562	-0.000057	2.312755	-1.079876	0.000262
C	3.614550	-1.035134	-0.000046	3.749006	-0.780052	0.000406
C	4.469611	-2.176099	-0.000111	4.664019	-1.895275	0.000400
C	3.850837	-3.492939	-0.000258	4.184598	-3.262457	0.000426
C	2.448362	-3.603406	-0.000174	2.798740	-3.487190	0.000346
C	1.615314	-2.486658	-0.000035	1.894760	-2.412310	0.000223
C	5.863466	-2.061792	0.000076	6.057723	-1.679803	0.000400
C	6.679558	-3.203242	0.000030	6.944675	-2.740216	0.000438
C	6.087854	-4.481784	-0.000227	6.481046	-4.076931	0.000486
C	4.712468	-4.628807	-0.000366	5.119806	-4.321605	0.000474
O	4.195604	0.166167	0.000367	4.151250	0.424337	0.000112
H	6.306662	-1.075409	0.000288	6.414776	-0.658387	0.000375
H	7.756647	-3.101063	0.000206	8.010525	-2.544765	0.000430
H	6.718771	-5.362859	-0.000267	7.185963	-4.897757	0.000516
H	4.270388	-5.618471	-0.000500	4.747997	-5.340500	0.000494
H	2.006458	-4.593396	-0.000218	2.417666	-4.500950	0.000329
H	0.542101	-2.620813	0.000039	0.835273	-2.649860	0.000072
H	-0.603298	-0.799517	0.000878	-0.557371	-0.833161	0.000058
H	-1.453714	1.598265	0.000513	-1.518621	1.531964	-0.000291
H	0.829805	3.145156	-0.000979	0.672604	3.194373	-0.000047
H	3.491809	0.873120	0.000818	2.755424	1.511464	0.000458

Table S5. Cartesian coordinates for the S₀-N_{syn} and S₀-PT forms of 3NI2OH shown in Fig. 4.

	S ₀ -N _{syn}			S ₀ -PT		
	x	y	z	x	y	z
C	-0.188059	-0.000035	-0.872843	-0.015577	0.006242	0.000225
H	1.846397	-0.000453	-0.192978	2.138055	-0.001389	-0.000465
C	0.799926	-0.000275	0.094647	1.237549	0.607260	-0.000065
C	-1.866614	0.000332	0.888940	-1.065071	2.203880	0.001180
C	0.509164	-0.000201	1.472616	1.386570	1.997447	-0.000242
C	-1.564233	0.000211	-0.455375	-1.246620	0.806946	0.001046
C	-0.863081	0.000101	1.876571	0.192321	2.806948	0.000340
C	1.522287	-0.000467	2.465917	2.659921	2.633401	-0.000944
H	-2.198750	0.000424	3.575576	-0.534594	4.846870	0.000911
H	-2.910627	0.000531	1.175995	-1.959285	2.815748	0.002197
C	1.199714	-0.000379	3.797886	2.768151	3.995591	-0.001031
H	2.560759	-0.000721	2.153388	3.550253	2.013112	-0.001417
H	1.980510	-0.000588	4.548017	3.741799	4.469673	-0.001582
C	-0.157293	-0.000061	4.198767	1.594395	4.798361	-0.000338
H	-0.402971	0.000004	5.253820	1.690704	5.877933	-0.000347
C	-1.160391	0.000181	3.264881	0.354320	4.226883	0.000362
O	-2.580166	0.000251	-1.339144	-2.406270	0.259472	0.003555
C	0.126261	0.000071	-2.295916	-0.183474	-1.415669	0.000134
N	1.381920	-0.000023	-2.834886	0.732039	-2.421090	0.001952
N	-0.775447	0.000410	-3.270428	-1.390224	-2.000867	-0.002561
C	-0.084042	0.000421	-4.454314	-1.254278	-3.368870	-0.001674
C	1.259473	0.000108	-4.207543	0.074573	-3.644308	0.001175
H	2.248445	-0.000556	-2.324415	1.729378	-2.290488	0.003834
H	-2.207461	-0.000013	-2.256328	-2.185594	-1.265798	-0.005266
H	-0.591384	0.000672	-5.404275	-2.100752	-4.031417	-0.003459
H	2.115657	0.000055	-4.858573	0.604559	-4.579111	0.002459

Table S6. Cartesian coordinates for the S₁-N_{syn} and S₁-PT forms of 3NI2OH shown in Fig. 4.

	S ₁ -N _{syn}			S ₁ -PT		
	x	y	z	x	y	z
C	0.069063	-0.052350	-0.000394	-0.023728	0.000114	0.014518
H	2.215134	0.035689	-0.000555	2.076383	-0.010782	-0.027644
C	1.294953	0.610068	-0.000411	1.169863	0.587876	-0.011215
C	-1.012358	2.197165	-0.000205	-1.124418	2.205521	-0.019444
C	1.422333	2.031124	-0.000515	1.319949	2.050001	0.094469
C	-1.115320	0.803018	-0.000096	-1.238861	0.809003	-0.109178
C	0.240125	2.851484	-0.000275	0.149309	2.850626	0.077389
C	2.664721	2.673816	-0.000645	2.554145	2.643832	0.272645
H	-0.533145	4.857402	-0.000247	-0.607485	4.859110	0.190113
H	-1.934034	2.765659	-0.000035	-2.031454	2.795341	-0.068374
C	2.764698	4.076709	-0.000681	2.673326	4.039481	0.384425
H	3.569557	2.077166	-0.000777	3.444682	2.026006	0.301261
H	3.745318	4.536369	-0.000807	3.652819	4.490097	0.481849
C	1.622738	4.868301	-0.000527	1.537972	4.830324	0.346844
H	1.700488	5.947368	-0.000569	1.620091	5.906640	0.433365
C	0.365647	4.252050	-0.000366	0.282215	4.240569	0.202208
O	-2.317271	0.262513	0.000156	-2.315084	0.197878	-0.395969
C	-0.117884	-1.458167	-0.000343	-0.309109	-1.481218	-0.075970
N	0.852414	-2.442643	-0.000438	0.616741	-2.500932	0.222605
N	-1.338411	-2.050815	-0.000253	-0.817270	-1.815729	-1.333765
C	-1.131682	-3.397398	-0.000231	-0.503258	-3.135826	-1.598170
C	0.207903	-3.674897	-0.000206	0.363216	-3.558773	-0.651123
H	1.846045	-2.299240	0.000015	0.877328	-2.684313	1.181038
H	-2.205869	-0.782301	0.000066	-1.694131	-1.322857	-1.536926
H	-1.951965	-4.095737	-0.000201	-0.859457	-3.650191	-2.473764
H	0.747380	-4.604711	-0.000195	0.864693	-4.505834	-0.551585

References

1. W. Guo, J. F. Li, N. J. Fan, W. W. Wu, P. W. Zhou and C. Z. Xia, *Synthetic Commun.*, 2005, **35**, 145-152.
2. W. H. Melhuish, *J. Phys. Chem.*, 1961, **65**, 229-235.